FUNCTIONAL ANALYSIS OF TROPOMYOSIN ISOFORMS IN VIVO

by

Aeri Cho

A dissertation submitted to Johns Hopkins University in conformity with the requirements for the degree of Doctor of Philosophy

Baltimore, Maryland

March, 2015

Abstract

Precise regulation of a dynamic actin cytoskeleton is an essential function of animal cells without which vesicle trafficking, cytokinesis, cell adhesion and cell movement would be impossible. Therefore, understanding the mechanisms underlying actin dynamics is fundamental for understanding basic cellular biology as well as gaining insight into mechanisms of embryonic development, tissue homeostasis and regeneration, and pathological processes such as inflammation and tumor metastasis.

Actin filaments are a major source of the protrusive and contractile forces that drive many cellular behaviors. Contractile forces require the action of non-muscle myosin II, which assembles onto actin filaments to form acto-myosin. The interaction between actin and myosin can occur spontaneously *in vitro,* but in cells it is regulated by accessory proteins including Tropomyosins (Tms). A complete understanding of Tm function has been elusive due in part to the large number of isoforms: 44 predicted isoforms from 4 genes in humans.

The goal of this study was to decipher the functional roles of different Tm isoforms at the molecular, cellular and tissue levels *in vivo*. *Drosophila* egg chambers are a genetically tractable system that expresses far fewer Tm isoforms than mammalian cells. We identified three tropomyosin isoforms expressed in follicle cells, including one previously annotated as muscle-specific. We generated and characterized isoform-specific antibodies, RNAi lines, and mutant alleles, and discovered that they function non-redundantly in the two cell types we studied: border cells, a well-studied example of collective migration, and epithelial follicle cells, which develop contractile stress fibers that shape the egg chamber.

We also found that Tm mutations interact genetically with Psidin, a conserved but poorly characterized protein that we found regulates lamellipodia dynamics in both *Drosophila* and mammalian cells. Although strong loss-of-function mutations in either Tm or Psidin inhibit border cell migration individually, mutation of Tm suppresses the Psidin mutant phenotype. Furthermore, in a biochemical assay, we showed that Psidin inhibited Tm protein binding to actin filaments. Taken together this work has generated reagents that will be generally useful in deciphering Tm isoform functions *in vivo* in *Drosophila*, has revealed isoform-specific functions, and has revealed a novel genetic and biochemical interaction.

Advisor: Dr. Denise J. Montell

Molecular, Cellular and Developmental Biology, UCSB

Reader: Dr. Douglas Robinson

Department of Cell Biology, Johns Hopkins School of Medicine

Acknowledgments

First and foremost, I would like to thank my advisor, Dr. Denise Montell. One of the best decisions I made in my life was to join her lab. Her original ideas and insights always fascinated me and made me wonder about science. She not only advised me to go forward with my project during hardships, but she also taught me to become more independent and more adventurous. I cannot thank enough for her decision to move to University of California, Santa Barbara and providing us with wonderful working environment. I am surely going to miss walks over to the beach and the beautiful weather.

I would like to thank past and present lab members of the Montell lab. Especially Adi Gurav for helping me out whenever I reached out for help. Also for enjoyable coffee breaks and moments of venting out when experiments did not work. Special thanks to Hsiang Chen and Leanna Li for delightful brunch conversations. I would also like to thank my undergraduate assistant, Tess Whitwam for her tremendous help and her commitment to lab work despite busy class schedule.

I would like to thank my thesis committee members Dr. Douglas Robinson, Dr. Susan Craig, and Dr. Deborah Andrew for their time and valuable advice on my project. Special thanks to Dr. Douglas Robinson, for reading my thesis and providing me lots of insights regarding my favorite protein, tropomyosin.

I would also like to thank parents for their endless love and support. They were always on my side and encouraged me to do whatever I pursued to do. I am happy that I could go back to Korea after 13 years of study in the states to spend the good times that I

have missed. Also big thanks to my brother and his family. Without my family's support, this dissertation would not have been possible.

Last but not least, I would like to thank my husband Jeonggil Ko. Although we have been apart longer than we have been together, there wasn't a single moment when I felt lack of attention or love. I thank him for being patient with me and for always encouraging me at times when I was discouraged with my research. Without him, I would not have made it to the end. We have been counting down the days till we meet and I am looking forward to the wonderful journey ahead of us.

Table of Contents

List of Figures

Chapter 1

Chapter 2

Chapter 3

List of Tables

Chapter 1: Introduction

Overview

The actin cytoskeleton is involved in crucial cellular activities, including cell migration, intracellular trafficking, cytokinesis, and many more. Therefore, understanding how the actin cytoskeleton is regulated is fundamental for a comprehensive understanding of basic cell biology. In this introduction, different actin structures such as lamellipodia protrusions, stress fibers, and adhesion complexes are introduced and their regulation by actin binding proteins are briefly described. These are summaries of well-characterized proteins and pathways from *in vitro* studies, using cell culture and biochemical assays. Although many findings from *in vitro* studies may be applied to reveal complex regulation *in vivo*, not much is known regarding *in vivo* regulation of the actin cytoskeleton. To begin to investigate this question, we first introduce our *in vivo* model system, the *Drosophila* egg chamber. I will specifically focus on border cell migration and our thorough knowledge on how collective cell migration is regulated. Lastly, I am going to introduce another tissue in the egg chamber, the epithelial follicle cells. While actin bundles in follicle cells of *Drosophila* egg chamber were observed a long time ago, these structures were not extensively studied until recently. Live imaging techniques and sophisticated genetic manipulations have revealed that the actin bundles are dynamic and that their regulation is tightly regulated by cell-cell interaction and cell-extracellular matrix interactions. Disruption in these interactions may cause changes in tissue shape and form.

I. Actin cytoskeleton

Different actin structures and cell migration

The human body is composed of more than 300 different cell types. These cell types not only have unique shapes, but also serve distinct functions, and proper function requires appropriate structure. The cytoskeleton, which is composed of microtubules, intermediate filaments, and actin filaments, plays a major role in regulating cellular architecture and function. Alterations in cytoskeletal morphology are characteristic of transformed cancer cells, neurological disorders, and other numerous diseases.

Actin is one of the most abundant proteins in eukaryotic cells. Actin filaments are dynamic. For example, dynamic actin structures, including lamellipodia, filopodia, focal adhesions, and stress fibers, play a major role during cell migration. Protrusion occurs in response to migratory or chemotactic stimuli in the region called lamellipodia where intricate branching and dynamic actin can be seen. Members of the Rho family of GTPases stimulate production of different types of actin structures. For example, the Rac GTPase activates the Arp2/3 complex and is involved in membrane ruffling in lamellipodia. Filopodia, are spike like protrusions regulated by Cdc42. Rho promotes stress fiber formation, such as transverse arcs and ventral stress fibers (Nobes and Hall, 1995) (Figure 1).

Stress fibers are composed of actin filaments bundled by actin binding proteins such as α-actinin. These contractile bundles end in focal adhesion complexes that connect actin filaments to the ECM (Naumanen et al., 2008). Stress fibers are easily seen in

cultured fibroblasts, smooth muscle, and many cancer cell lines. In these cultured cells, different kinds of stress fibers can be seen depending on their localization and function and can be categorized as dorsal, ventral, or transverse arcs. A defining feature of stress fibers is their contractility, which is controlled by ATP-driven myosin. Phosphorylation of the myosin light chain is required for this contractility; this is controlled by at least two independent pathways: Ca^{2+}/calmodulin and Rho dependent. Ca^{2+}/calmodulin activates the myosin light chain kinase (MLCK), which then phosphorylates the myosin light chain. Rho GTPase either directly phosphorylates the myosin light chain or is involved indirectly, by inhibiting the activity of phosphorylation of myosin light chain phosphatase (Katoh et al., 2001a; Katoh et al., 2001b). Recent studies show that stress fibers also contain distinct tropomyosin isoforms with non-redundant functions to recruit the myosin light chains (Tojkander et al., 2011). However, the detailed contributions of tropomyosin isoforms to actomyosin function in distinct cell types *in vivo* remain to be elucidated.

Different actin binding proteins and their functions

To date, at least 160 actin-binding proteins have been identified to function in regulating actin monomers, actin filament turnover, and higher order actin filament formation. Actin monomers (G-actin) spontaneously assemble into double helical filaments (F-actin). The building of actin filaments is asymmetric, with one fast growing end (barbed end) and one end with higher depolymerizing activity (pointed end). Actin polymerization and depolymerization are tightly regulated by actin binding proteins (Figure 2).

Extracellular signaling such as growth factors, cytokines, and hormones bind to surface receptors that activate intracellular Rho GTPases such as Rho, Rac and Cdc42. Downstream effectors of Rho GTPases are known as nucleation promoting factors (NPF), such as WASP/WAVE, which play a crucial role in nucleating Arp 2/3 complexes. Activated Arp2/3 complex binds to existing actin filaments to promote new branch formation. Due to abundant Arp2/3 complexes and actin polymerization activity, many branched actin filamentous networks are observed right beneath the leading edge of a protruding cell. These new filaments and their polymerization provide force for membrane protrusion. Capping proteins bind to barbed ends of actin filaments to inhibit addition or loss of actin monomers. Profilin, a G-actin binding protein, promotes ADP-ATP exchange of G-actin and its addition at barbed ends, facilitating actin polymerization. Depolymerization occurs at the pointed end of the actin filament. Severing activity of cofilin is important not only for regulation of depolymerization, but also for continued rapid growth in the barbed end, as dissociated actin subunits replenish the pool of free monomers. In addition, severing provides new barbed ends and new sites available for branching activity, further promoting dynamics in the actin network (DesMarais et al., 2005) The polymerized actin filaments are stabilized by Tropomyosin, which forms coiled-coil dimers and binds to the actin filament to inhibit actin filament depolymerization. The stabilized filaments are bundled into higher order structures with the help of bundling or crosslinking proteins such as fascin, fimbrin, and α-actinin.

Much knowledge has been accumulated about the regulation of actin filaments during cell migration *in vitro*. Utilizing cell cultures and biochemical assays has been successful to identify many actin-regulating proteins. Although these *in vitro* studies are

indispensable, cells do not all behave as is observed in cell cultures, so we set out to investigate the functions of Tm isoforms *in vivo* using the *Drosophila* ovary as a model.

II. Drosophila egg chamber as a model organism

Border cell migration

Drosophila females have two ovaries, each composed of ~16 ovarioles. The ovariole is a string of developing egg chambers from the tip – the germarium - where the follicle stem cells and germline stem cells reside, to the final product, the egg (Figure 3). In between there are 14 stages of egg chamber development. Each egg chamber contains 16 germline cells surrounded by an epithelium composed of somatic follicle cells. During stage nine, six to 10 follicle cells called border cells form a cluster and delaminate from the anterior of the egg chamber, migrate in between the nurse cells, and reach the border of the oocyte by stage 10. Later, these cells participate in making the micropyle, a structure that is required for sperm entry (Montell et al., 1992). Thus, incomplete border cell migration results in female sterility.

The border cell cluster contains two non-migratory polar cells in the middle surrounded by six to eight migratory cells. The polar cells secrete the cytokine Unpaired, which activates JAK/STAT signaling and specifies the migratory fate (Silver and Montell, 2001). Ectopic polar cells induce neighboring cells to form migratory border cells (Bai and Montell, 2002; Liu and Montell, 1999). STAT activates 200 or more direct and indirect downstream target genes such as slbo, armadillo (*Drosophila* β-catenin), and

DE-cadherin, which are required for migration. The JAK/STAT maintains both cell fate and motility (Montell, 2003). These were the first studies to implicate JAK/STAT signaling in motility. Subsequent studies have confirmed this role for JAK/STAT in ovarian (Silver et al., 2004) and prostate cancer and in a variety of normal, developmental migrations (Hou et al., 2002).

The timing of cluster formation and delamination is determined by a steroid hormone called Ecdysone and a steroid hormone receptor co-activator, Taiman. Ecdysone level surges in stage 9 when border cells start to delaminate and peaks at stage 10 when border cells reach the oocyte. Defects in Taiman or level of Ecdysone cause border cell migration defect (Bai et al., 2000; Jang et al., 2009).

For collective migration, border cells must first maintain the cluster through cell-cell adhesions, a major component of which is a protein called DE-cadherin. Early studies show that disruption in DE-cadherin activity in border cells or the nurse cells results in border cell migration defect (Niewiadomska et al., 1999) however the reasons for the defect were unclear. Recently, DE-cadherin's has been shown to play three distinct roles in promoting the collective directional migration of the border cell cluster (Cai et al., 2014). Specifically, DE-cadherin and Rac are involved in a positive feedback loop to amplify guidance receptor signaling at the leading edge, which promotes forward-directed border cell migration. Secondly, DE-cadherin in junctions between individual migrating border cells mechanically couples the leading cell to the following cells which is necessary for communication of directional information. Thirdly, DE-cadherin functions in between polar cells and outer, migratory cells to hold the cluster together.

Actin regulatory pathways are also involved during border cell migration. When the border cells migrate, the cluster extends prominent forward-directed protrusions (Fulga and Rorth, 2002; Prasad and Montell, 2007). Rac activity in the leader cell of the border cell cluster is required for directional border cell migration (Murphy and Montell, 1996; Wang et al., 2010). Many other actin-regulating proteins found to function in single cell migration in cultured cells were also shown to play a role in border cell migration *in vivo*. For example, Profilin, a conserved protein known to bind to actin monomers, promotes protrusions in border cells (Verheyen and Cooley, 1994). Cofilin is required for actin turnover and lamellipodial protrusion of border cells (Chen et al., 2001; Zhang et al., 2011). Other actin regulators such as SCAR/WAVE, Arp2/3, and Enabled were also found to play intricate roles in border cell migration (Gates et al., 2009; Poukkula et al., 2014)

Epithelial follicle cells – organization and regulation

The *Drosophila* egg chamber is composed of 16 germline cells enclosed in approximately 1000 somatic follicle cells. The germ cells differentiate into 15 nurse cells and one oocyte, which later develops into an egg. The follicle cells secrete eggshell proteins and patterning signals to the oocyte, which is required for normal embryo development (Poulton and Deng, 2007).

During oogenesis, the follicle cells experience dramatic changes in their morphology. The follicle cells are cuboidal as egg chambers emerge from the germarium. However, as the egg chamber develops, the follicle cells show collective migration

towards the oocyte, forming a columnar shape while the anterior follicle cells flatten to form a squamous shape to enclose the nurse cells.

The epithelial follicle cells are polarized, with the apical side facing the oocyte and the basal layer touching the extracellular matrix (ECM) (Figure 4). The cell-ECM interaction occurs in focal adhesion complexes localized near the basal surface of the follicle cells with their associated, contractile F-actin bundles.

A few actin filaments can be observed near the basal surfaces of these follicle cells as the egg chambers bud from the germarium. However, at stage five the actin filaments assemble to form more obvious noticeable fibers. These fibers constantly go through disassembly and reassembly to form parallel arrays perpendicular to the anterior-posterior axis during stage 7, and by stage 12, they form thick bundles (Delon and Brown, 2009). The actin bundles end in focal adhesion-like structures that mediate follicle cell attachment to the basal lamina. Moreover, the actin fibers bind myosin, which induces contractile force along the actin fibers. We refer to these fibers as stress fibers (Wang and Riechmann, 2007), as their appearance and function are very similar to stress fibers found in cell cultures.. Additionally, many factors regulating stress fibers have been identified *in vitro*. However, stress fibers have rarely been detected in living tissue, thus making it nearly impossible to study the functions and regulations of stress fiber *in vivo*. Therefore, *Drosophila* follicle cells, with distinguishable stress fibers and live imaging techniques, along with the organism's genetic tractability, make a favorable system to investigate stress fiber regulation *in vivo*. Using this system, several proteins have been identified to play a role in formation and organization of the parallel actin filaments. Mutation in Pak (p21-activated kinase), a serine/threonine kinase that is

activated by the Rho GTPase pathway, causes loss of actin filaments in the follicle cells (Conder et al., 2007). Reduction in Talin, a protein that mediates cell-ECM adhesion, also results in reduction of actin fibers and loss of parallel organization (Becam et al., 2005).

How tissues shape their form and structure - Egg chamber rotation and elongation

How cellular components organize themselves to form specific shapes and sizes has been a major fundamental question asked throughout the study of development. The *Drosophila* egg chamber is a relatively simple system to study how tissues form their shape and structure. Egg chambers bud off from the germarium as a sphere, but soon undergo dramatic changes, elongating so that by stage 10, the egg chamber is 2.5 times longer than it is wide. Different mechanisms underlie egg chamber elongation during oogenesis. Initially, the follicle epithelial cells show collective migration along the surrounding basal lamina, which causes the egg chamber to rotate, providing force for initial egg chamber elongation (Haigo and Bilder, 2011). Recently, it has been reported that egg chambers start to rotate as early as stage one and slowly continues until roughly stage 6 where its rotation speed increases (Cetera et al., 2014). In this study, Cetera et al. show that early rotation is required for tissue-level actin bundle alignment. Follicle cells with defects in integrin or proteins that mediate interaction between the basal actin cytoskeleton and the ECM also show disturbed actin bundle alignment, which may constrain egg chambers from elongating (Bateman et al., 2001; Frydman and Spradling, 2001).

During stage 9, the rotation of the egg chamber gradually ceases and myosin oscillation on the basal actin fibers further elongates the egg chambers (He et al., 2010). Disturbing or enhancing the link between the actin cytoskeleton and the ECM alters myosin oscillation, thus affecting egg chamber elongation. These examples show that the egg chambers utilize at least two different mechanisms during their development to elongate and form their final shape.

Thesis Overview

My thesis focuses on using *Drosophila* egg chambers as a model system to study the intricate functions of tropomyosin *in vivo*. At least 44 isoforms are expressed in the mammalian system creating an obstacle to researchers studying the mechanisms of tropomyosin action *in vivo*.

In Chapter II, I introduce my study of mammalian tropomyosin and research on isoform-specific functions of *Drosophila* Tropomyosin1 using the border cell migration system and the actin stress fibers at the basal surface of epithelial follicle cells. Our results suggest that Tropomyosin1 isoforms expressed in the egg chamber have non-redundant roles that are involved in both processes.

In Chapter III, I describe the study of Psidin, a conserved but poorly characterized protein that was discovered in a genetic screen for mutations that disrupt border cell migration and which regulates lamellipodia dynamics in both Drosophila and mammalian cells. In this study, we found that Psidin and Tropomyosin1 have antagonizing functions in the regulation of actin dynamics.

Reference

Bai, J., and Montell, D. (2002). Eyes absent, a key repressor of polar cell fate during Drosophila oogenesis. Development *129*, 5377-5388.

Bai, J., Uehara, Y., and Montell, D.J. (2000). Regulation of invasive cell behavior by taiman, a Drosophila protein related to AIB1, a steroid receptor coactivator amplified in breast cancer. Cell *103*, 1047-1058.

Bateman, J., Reddy, R.S., Saito, H., and Van Vactor, D. (2001). The receptor tyrosine phosphatase Dlar and integrins organize actin filaments in the Drosophila follicular epithelium. Current biology : CB *11*, 1317-1327.

Becam, I.E., Tanentzapf, G., Lepesant, J.A., Brown, N.H., and Huynh, J.R. (2005). Integrin-independent repression of cadherin transcription by talin during axis formation in Drosophila. Nature cell biology *7*, 510-516.

Cai, D., Chen, S.C., Prasad, M., He, L., Wang, X., Choesmel-Cadamuro, V., Sawyer, J.K., Danuser, G., and Montell, D.J. (2014). Mechanical feedback through E-cadherin promotes direction sensing during collective cell migration. Cell *157*, 1146-1159.

Cetera, M., Ramirez-San Juan, G.R., Oakes, P.W., Lewellyn, L., Fairchild, M.J., Tanentzapf, G., Gardel, M.L., and Horne-Badovinac, S. (2014). Epithelial rotation

promotes the global alignment of contractile actin bundles during Drosophila egg chamber elongation. Nature communications *5*, 5511.

Chen, J., Godt, D., Gunsalus, K., Kiss, I., Goldberg, M., and Laski, F.A. (2001). Cofilin/ADF is required for cell motility during Drosophila ovary development and oogenesis. Nature cell biology *3*, 204-209.

Conder, R., Yu, H., Zahedi, B., and Harden, N. (2007). The serine/threonine kinase dPak is required for polarized assembly of F-actin bundles and apical-basal polarity in the Drosophila follicular epithelium. Developmental biology *305*, 470-482.

Delon, I., and Brown, N.H. (2009). The integrin adhesion complex changes its composition and function during morphogenesis of an epithelium. Journal of cell science *122*, 4363-4374.

DesMarais, V., Ghosh, M., Eddy, R., and Condeelis, J. (2005). Cofilin takes the lead. Journal of cell science *118*, 19-26.

Frydman, H.M., and Spradling, A.C. (2001). The receptor-like tyrosine phosphatase lar is required for epithelial planar polarity and for axis determination within drosophila ovarian follicles. Development *128*, 3209-3220.

Fulga, T.A., and Rorth, P. (2002). Invasive cell migration is initiated by guided growth of long cellular extensions. Nature cell biology *4*, 715-719.

Gates, J., Nowotarski, S.H., Yin, H., Mahaffey, J.P., Bridges, T., Herrera, C., Homem, C.C., Janody, F., Montell, D.J., and Peifer, M. (2009). Enabled and Capping protein play important roles in shaping cell behavior during Drosophila oogenesis. Developmental biology *333*, 90-107.

Haigo, S.L., and Bilder, D. (2011). Global tissue revolutions in a morphogenetic movement controlling elongation. Science *331*, 1071-1074.

He, L., Wang, X., Tang, H.L., and Montell, D.J. (2010). Tissue elongation requires oscillating contractions of a basal actomyosin network. Nature cell biology *12*, 1133-1142.

Hou, S.X., Zheng, Z., Chen, X., and Perrimon, N. (2002). The Jak/STAT pathway in model organisms: emerging roles in cell movement. Developmental cell *3*, 765-778.

Jang, A.C., Chang, Y.C., Bai, J., and Montell, D. (2009). Border-cell migration requires integration of spatial and temporal signals by the BTB protein Abrupt. Nature cell biology *11*, 569-579.

Katoh, K., Kano, Y., Amano, M., Kaibuchi, K., and Fujiwara, K. (2001a). Stress fiber organization regulated by MLCK and Rho-kinase in cultured human fibroblasts. American journal of physiology Cell physiology *280*, C1669-1679.

Katoh, K., Kano, Y., Amano, M., Onishi, H., Kaibuchi, K., and Fujiwara, K. (2001b). Rho-kinase--mediated contraction of isolated stress fibers. The Journal of cell biology *153*, 569-584.

Liu, Y., and Montell, D.J. (1999). Identification of mutations that cause cell migration defects in mosaic clones. Development *126*, 1869-1878.

Montell, D.J. (2003). Border-cell migration: the race is on. Nature reviews Molecular cell biology *4*, 13-24.

Montell, D.J., Rorth, P., and Spradling, A.C. (1992). slow border cells, a locus required for a developmentally regulated cell migration during oogenesis, encodes Drosophila C/EBP. Cell *71*, 51-62.

Murphy, A.M., and Montell, D.J. (1996). Cell type-specific roles for Cdc42, Rac, and RhoL in Drosophila oogenesis. The Journal of cell biology *133*, 617-630.

Naumanen, P., Lappalainen, P., and Hotulainen, P. (2008). Mechanisms of actin stress fibre assembly. Journal of microscopy *231*, 446-454.

Niewiadomska, P., Godt, D., and Tepass, U. (1999). DE-Cadherin is required for intercellular motility during Drosophila oogenesis. The Journal of cell biology *144*, 533-547.

Nobes, C.D., and Hall, A. (1995). Rho, rac and cdc42 GTPases: regulators of actin structures, cell adhesion and motility. Biochemical Society transactions *23*, 456-459.

Poukkula, M., Hakala, M., Pentinmikko, N., Sweeney, M.O., Jansen, S., Mattila, J., Hietakangas, V., Goode, B.L., and Lappalainen, P. (2014). GMF promotes leading-edge dynamics and collective cell migration in vivo. Current biology : CB *24*, 2533-2540.

Poulton, J.S., and Deng, W.M. (2007). Cell-cell communication and axis specification in the Drosophila oocyte. Developmental biology *311*, 1-10.

Prasad, M., and Montell, D.J. (2007). Cellular and molecular mechanisms of border cell migration analyzed using time-lapse live-cell imaging. Developmental cell *12*, 997-1005.

Silver, D.L., and Montell, D.J. (2001). Paracrine signaling through the JAK/STAT pathway activates invasive behavior of ovarian epithelial cells in Drosophila. Cell *107*, 831-841.

Silver, D.L., Naora, H., Liu, J., Cheng, W., and Montell, D.J. (2004). Activated signal transducer and activator of transcription (STAT) 3: localization in focal adhesions and function in ovarian cancer cell motility. Cancer research *64*, 3550-3558.

Tojkander, S., Gateva, G., Schevzov, G., Hotulainen, P., Naumanen, P., Martin, C., Gunning, P.W., and Lappalainen, P. (2011). A molecular pathway for myosin II recruitment to stress fibers. Current biology : CB *21*, 539-550.

Verheyen, E.M., and Cooley, L. (1994). Profilin mutations disrupt multiple actin-dependent processes during Drosophila development. Development *120*, 717-728.

Wang, X., He, L., Wu, Y.I., Hahn, K.M., and Montell, D.J. (2010). Light-mediated activation reveals a key role for Rac in collective guidance of cell movement in vivo. Nature cell biology *12*, 591-597.

Wang, Y., and Riechmann, V. (2007). The role of the actomyosin cytoskeleton in coordination of tissue growth during Drosophila oogenesis. Current biology : CB *17*, 1349-1355.

Zhang, L., Luo, J., Wan, P., Wu, J., Laski, F., and Chen, J. (2011). Regulation of cofilin phosphorylation and asymmetry in collective cell migration during morphogenesis. Development *138*, 455-464.

Figure 1. A schematic diagram of migrating single cell

A migrating cell shows polarized morphology, with leading edge showing protrusions and filopodia. Branched actin network is observed in the lamellipodia, actin polymerization pushing the membrane towards the direction of migration. New adhesions to the substrate form near the leading edge while cell-substrate interaction is dissociated in the rear of the cell, allowing the cell to retract. Different classes of stress fibers recruit myosin II and generate contractile force. Some studies show that different tropomyosin isoforms bind to different classes of stress fibers.

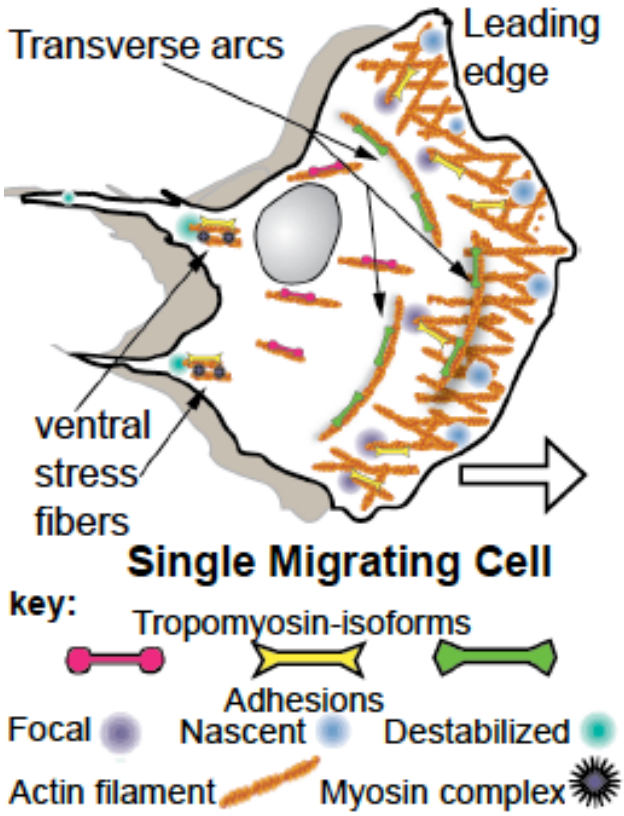
Transverse arcs
Leading edge
ventral stress fibers
Single Migrating Cell
key:
Tropomyosin-isoforms
Adhesions
Focal
Nascent
Destabilized
Actin filament
Myosin complex

Figure 2. Actin binding proteins during cell migration

When a cell receives extracellular stimuli, the information is relayed to Rho GTPases inside the cell. Activated Rho GTPases activate WASP/Scar, which is required for Arp2/3 complex nucleation. Arp2/3 promotes branch formation and new actin polymerization occurs at new branch sites. Profilin binds to G-actin and promotes ADP-ATP exchange of G-actin and addition of actin monomers to the barbed end. Actin polymerization pushes the membrane, which is required for protrusion formation during cell migration. The polymerization at the barbed end of the actin filament is impeded by binding of capping proteins and at the same time, the loss of actin monomers is prevented. Depolymerization and severing occurs near the pointed end of the actin filament by ADF/cofilin. The actin filament is stabilized by Tropomyosin and Fimbrin, while Fascin bundles filaments to make a higher order structure.

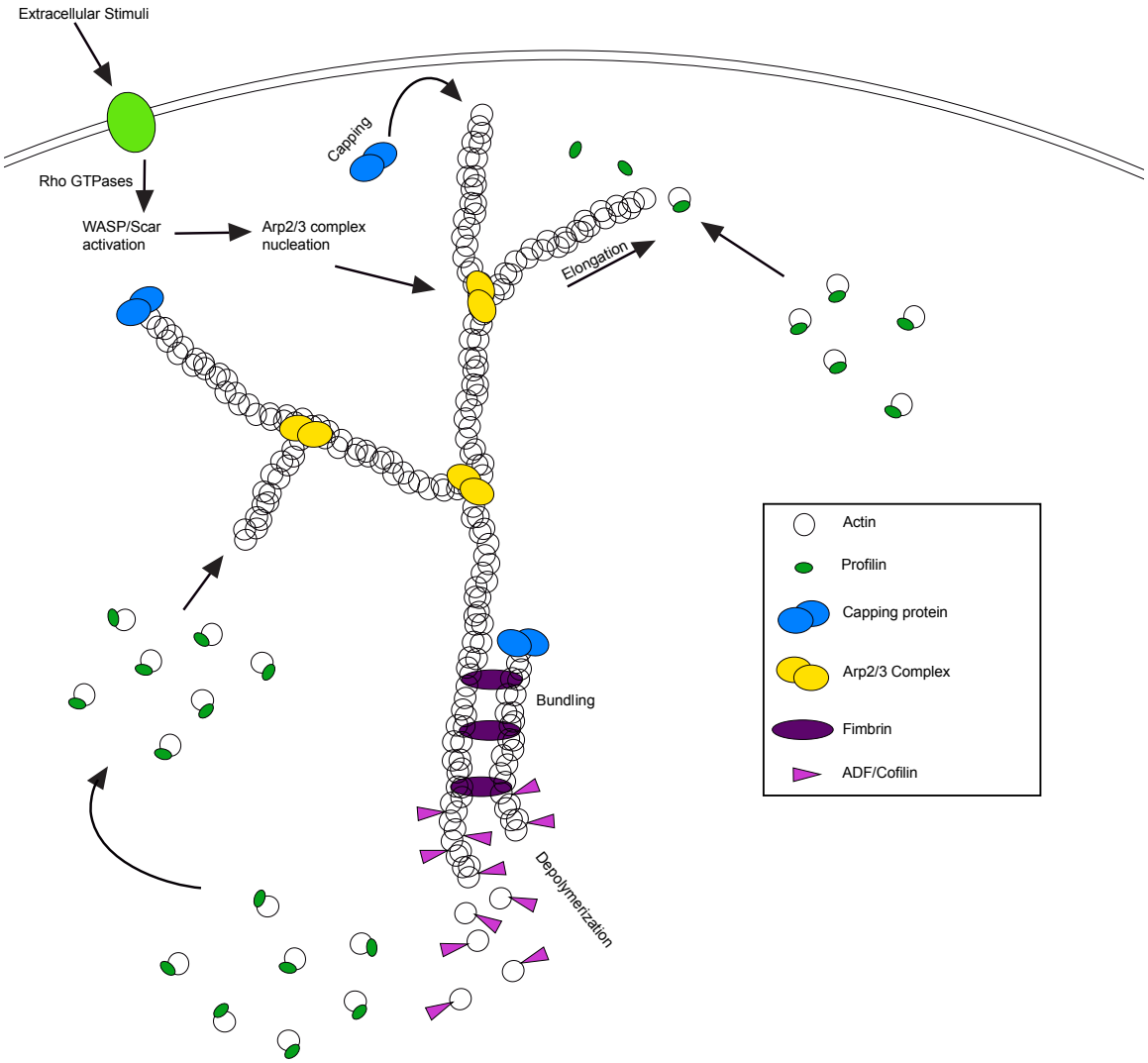
Extracellular Stimuli
Rho GTPases
WASP/Scar activation
Arp2/3 complex nucleation
Capping
Elongation
Bundling
Depolymerization
Actin
Profilin
Capping protein
Arp2/3 Complex
Fimbrin
ADF/Cofilin

Figure 3. *Drosophila* ovaries and egg chamber development

A schematic drawing of a female *Drosophila* and two ovaries, which consists of strings of developing egg chambers called ovarioles. Somatic follicle cells enclose 15 nurse cells and one oocyte, which are derived from germline stem cells. Newly synthesized egg chambers bud off from the germarium with the stalk cells (purple) connecting egg chambers in developing stages. In stage 9 egg chambers, a cluster of migratory cells called border cells (blue) containing non-migratory polar cells in the middle (pink) delaminate from the anterior of the egg chamber and migrate in between the nurse cells to reach the oocyte. The migration process is completed at stage 10.

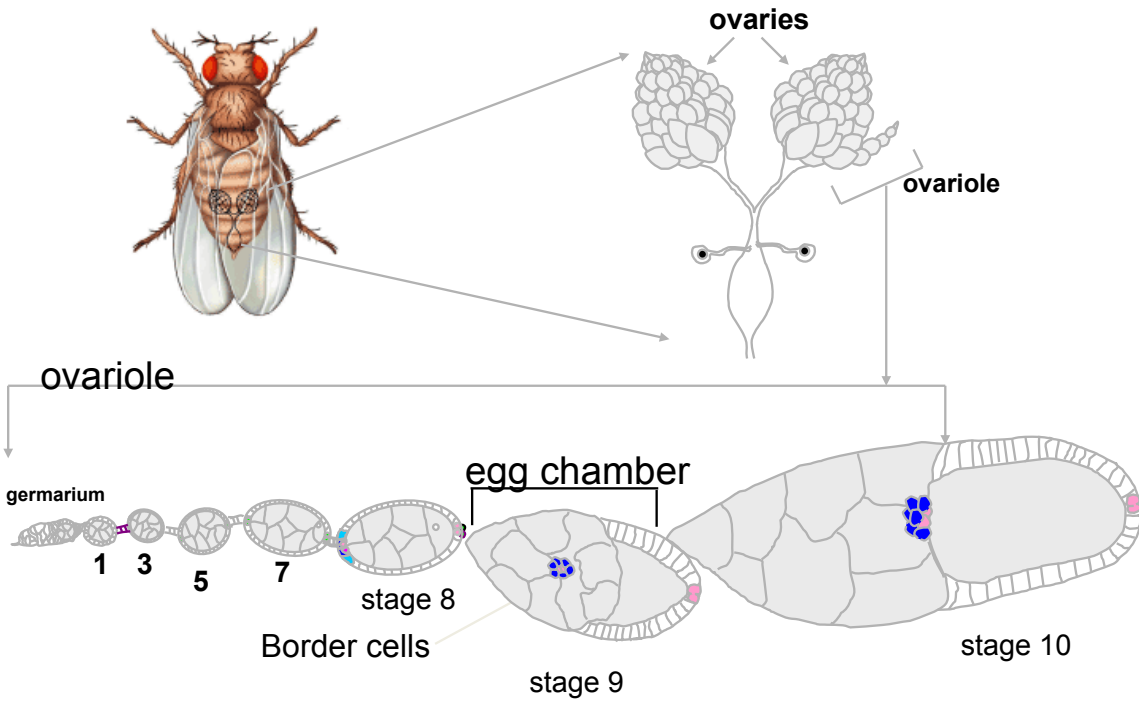
ovaries
ovariole
ovariole
germarium
1
3
5
7
egg chamber
stage 8
Border cells
stage 9
stage 10

Figure 4. Drosophila egg chamber epithelial follicle cells

(**A**) Drosophila epithelial follicle cells are polarized. The basal layer interacts with the extracellular matrix (ECM, shown in green) and the apical side faces the oocyte.

(**B**) Close up view of three follicle cells show polarized follicle cells connected with adherens junction, and basal actin underlying the basal layer. This very thin structure (~1um) can be seen at the outer layer of the egg chamber, right beneath the coverslip.

(Images adapted from He et al., 2010)

(**C**) Confocal micrograph of a stage 10 egg chamber is shown below the depicted diagram. Non-muscle myosin light chain is expressed in red and the focal adhesion complex protein paxillin is marked in green.

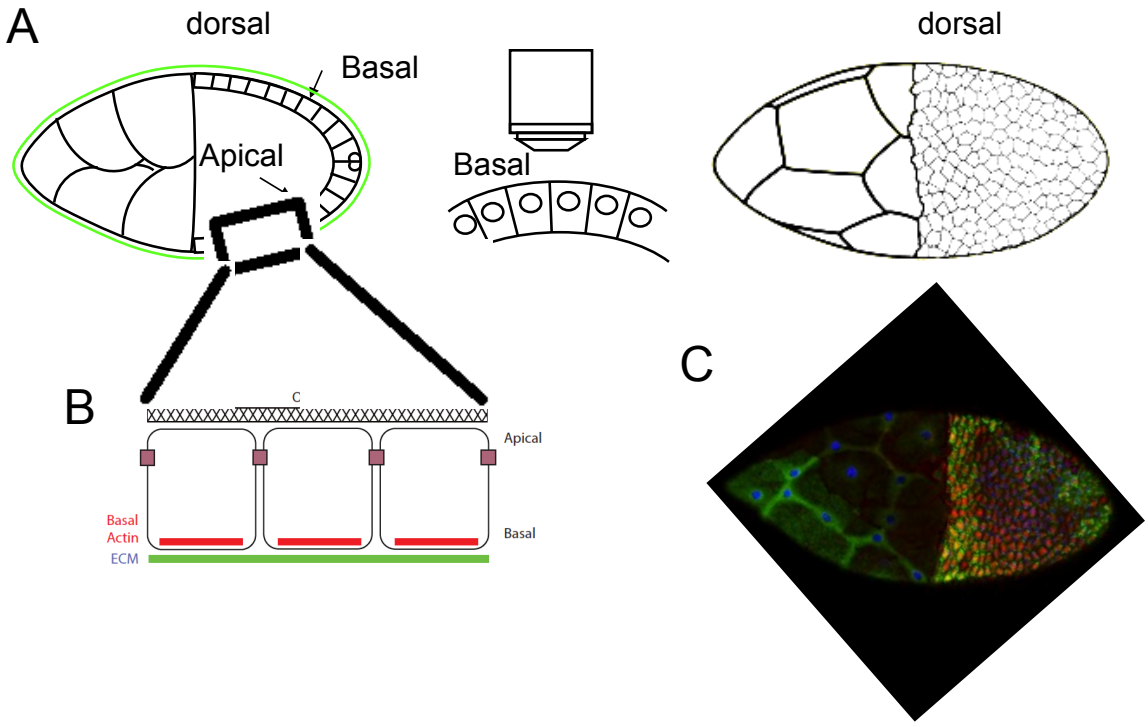
A
dorsal
Basal
Apical
Basal
dorsal
B
C
Apical
Basal
Actin
ECM
Basal
C

Chapter 2:
Functional analysis of Tropomyosin isoforms *in vivo*

Introduction

Tropomyosin in mammalian system

Tropomyosin (Tm) is a key regulator of actin filaments. Tm is a coiled coil dimer that binds head to tail to form a polymer. Tm was first identified in striated muscles, where it is required for regulating muscle contraction (Bailey, 1946). Specifically, Tm dimers form a complex with Troponin (Tn) that binds along the actin filament. In the absence of Ca^{2+}, Tm-Tn complex masks the myosin binding site along the actin filament. An increase in the Ca^{2+} level inside the cell, followed by Ca^{2+}binding to the Tn-Tm complex causes it to undergo a conformational change, thus allowing the myosin to bind actin, which is required for subsequent acto-myosin contraction. Since its discovery, the role of Tm in acto-myosin contraction in muscle cells has been extensively studied and its function has been well characterized. Recently, the structure of the actin-Tm-myosin complex in its active and inactive states has been determined by cyro-electron microscopy (Behrmann et al., 2012; von der Ecken et al., 2014)

Interestingly, Tm is not only expressed in muscle cells, but is also abundant in the cytoskeleton of non-muscle cells (Talbot and MacLeod, 1983). Although muscle Tm has been extensively studied, functional studies of non-muscle Tm are relatively new. Since the Troponin complex is absent in non-muscle cells, acto-myosin contractions via Tn-Tm do not occur. Two functions of Tm *in vitro* in non-muscle cells are to stabilize actin filaments in the lamella area and to interact with other actin binding proteins to regulate actin dynamics. However, not much is known regarding its actin regulation *in vivo*.

Study of Tm in the mammalian system *in vivo* is complicated due to the expression of at least 44 isoforms. In mammalian cells, four structurally similar Tm genes exist, suggesting that they arose from duplications of an ancestral gene. These genes encode more than 40 different isoforms through the use of alternate promoters and alternative splicing (Gunning et al., 2008). Tm isoforms are conventionally categorized into low molecular weight (LMW:~248 amino acids) and high molecular weight (HMW:~284 amino acids) according to their molecular masses. Both HMW and LMW isoforms can be expressed from the same gene. Tms may also form heterodimers, adding further complexity to the array of possible functional proteins (Gimona et al., 1995).

Tm mRNAs are differentially expressed in human tissues such as fibroblasts, smooth muscle, and intestinal epithelia (Novy et al., 1993). Moreover, isoform expression can change during muscle differentiation, embryogenesis, and neuronal differentiation, processes accompanied by morphological changes (Gunning et al., 1990; Muthuchamy et al., 1993; Weinberger et al., 1993). In neurons, Tm isoform expression is spatially and temporally regulated (Schevzov et al., 2005), such that the isoform Tm3 is broadly expressed, whereas Tm5NM1 is enriched in filopodia and growth cones. These examples highlight that tissue-specific isoform expression is highly complex and regulated both spatially and temporally.

Non-muscle Tropomyosin as a regulator of actin cytoskeleton

In vitro, non-muscle Tm inhibits Arp2/3-dependent actin filament branching activity (Blanchoin et al., 2001) and antagonizes the actin filament severing activity of cofilin

(Ono and Ono, 2002). The simple view is that Tm functions to stabilize actin filaments by inhibiting branching and depolymerization. However, many Tm isoforms exist, which may have redundant or non-redundant roles or even antagonistic roles in actin dynamic regulation. For example, isoforms Tm5NM1 and Tm3 were shown to have antagonistic functions. These two isoforms also showed opposite sensitivity to actin-depolymerizing drugs (Creed et al., 2011)

The well-studied, non-muscle isoform Tm5NM1 functions in recruiting myosin II, resulting in actin filament tension (Bryce et al., 2003). When the same isoform is overexpressed, it inhibits Src activation and stabilizes mature focal adhesions. On the other hand, when Tm5NM1 is depleted in cultured cells, Rac dependent lamellipodia are enhanced, increasing cell motility (Bach et al., 2009). Recently, new roles of non-muscle Tm have been identified, such as functions in asymmetric cell division, filopodia formation, and contributing to contractile forces at the zonula adherens (Caldwell et al., 2014; Creed et al., 2011; Jang et al., 2014). However, most of these studies were done *in vitro*, and not much is known regarding the *in vivo* functions of non-muscle Tm.

Importance of studying Tropomyosin regulation

Tm is an essential gene that causes lethality when knocked out in yeast, worms, flies, and mammals. In addition decreased expression of HMW Tms is a hallmark of transformed cells (Hendricks and Weintraub, 1981). HMW isoforms Tm1 and Tm2 are normally associated with stress fibers, but are either downregulated or lost during malignant transformation; additionally, the cells showed highly metastatic behavior. On the other

hand, some LMW Tms are reported to show elevated levels up to 1.5~1.8 fold in invasive cancer cells (Miyado et al., 1997). In addition, recent studies report that some Tm isoforms show elevated levels during the epithelial-mesenchymal transition in lens epithelial cells (Kubo et al., 2013)

Distinct Tm isoforms may serve unique functions in different parts of the cell (Creed et al., 2008), suggesting that drugs that target specific Tm isoforms characteristic of transformed cells might show more specific anti-tumor activities than drugs targeting actin itself, which are highly toxic. Recently, there has been an attempt to apply this idea. Anticancer compound TR100 was designed to target one of the non-muscle Tm isoforms, Tm5NM1. It was shown that TR100 selectively affects actin filaments that are associated with Tm5NM1, *in vivo* and *in vitro*, without compromising cardiac activity or other types of actin filaments. (Stehn et al., 2013) However, a more thorough understanding of Tm regulation is required for further application.

Drosophila Tropomyosin

Drosophila has two Tm genes, Tm1 and Tm2, that are closely linked on chromosome 3 and show an average of about 47% identity with vertebrate Tms (Bautch et al., 1982). Tm2, which encodes six isoforms, is expressed in indirect flight muscles and in cardiac muscles. Tm1 encodes 17 different isoforms, via alternative splicing. Among them, 11 are annotated as muscle-specific, while six are predicted to be expressed under the control of the non-muscle promoter (Hanke and Storti, 1988) (Figure 1).

Mutations in Drosophila Tm1 are homozygous lethal and cause defects in head morphogenesis during development (Tetzlaff et al., 1996), the size of dendritic fields in neurons (Li and Gao, 2003), and oskar mRNA mis-localization in oocytes (Erdelyi et al., 1995). However, which of the 17 isoforms is required for each of these functions remains unclear since not all isoforms were annotated until recently. Moreover, there were no specific antibodies to detect the isoforms, and it was unclear which isoforms were affected or unaffected by existing mutant alleles.

The *Drosophila* genome appears to encode structurally unusual forms of Tm, which until now has been classically defined as an end-to-end coiled-coil dimer. While most *Drosophila* Tm1 isoforms are predicted to form a coiled-coil structure from the N- to the C-termini, Tm1-I, Tm1-C, and Tm1-H isoforms possess a long unstructured N-terminal tail, coiled-coil only in the middle, and a second unstructured stretch of amino acids at the C-terminus (Figure 2). The fact that many Tm1 isoforms exist and that each Tm1 isoform shows different amino acid sequence may indicate that each isoform serves a unique function. The main purpose of my study is to elucidate functions of different Tm1 isoforms. *Drosophila's* fewer Tm isoforms and genetic tractability offer a relatively simple system for deciphering the functions of different Tm1 isoforms.

Results

Three Tropomyosin isoforms are expressed in the *Drosophila* egg chamber

Study of *Drosophila* tropomyosin (Tm1) has been limited due its complex regulation by many spliced isoforms. To determine which of the 17 isoforms are expressed in follicle cells of the egg chamber, we performed an mRNA tagging experiment (Yang et al., 2005). Briefly, flies expressing a follicle-cell-specific Gal4 driver were crossed with flies expressing flag-tagged poly A binding protein (PABP) under UAS promoter. The ovaries from the progeny were dissected, homogenized and subjected to an anti-FLAG pull-down assay. The flag-tagged mRNA, which was specifically expressed in the follicle cells of interest, was isolated and used for RT-PCR. Using specific primers, we detected only Tm1-A, Tm1-I and Tm1-L isoforms in each follicle cell population tested, including polar cells (Upd-Gal4), border cells (slbo-Gal4) and all follicle cells (Cy2-Gal4). For a positive control, we isolated mRNA from whole ovaries from the same genotype and performed the same treatment apart from the flag-tag pull-down. From the control mRNA, we were able to amplify many additional isoforms including muscle type (Tm1-J, Tm1-N, Tm1-O, Tm1-M, Tm1-S), Tm1-C, and Tm1-Q as well as Tm1-A, Tm1-I, Tm1-L and Tm1-P (Figure 3). The presence of the L isoform in follicle cells was surprising because it had previously been annotated as muscle-specific. These results suggested that Tm1-A, Tm1-L and Tm1-I were the predominant Tm1 isoforms expressed in all follicle cell populations including polar cells and border cells.

Analysis of different Tm1 isoforms in the egg chambers using isoform specific antibodies

During our search for suitable *Drosophila* Tm1 antibodies, we came upon a monoclonal antibody commercially available from Abcam. The antibody was generated using purified Tm-Tn complex from a species called *Lethocerus* (Waterbug) as an antigen. The antibody is known to detect invertebrate flight or indirect flight muscle and was previously used in numerous studies to study *Drosophila* muscle regulation. However it was not clear whether the epitope was Tm or Tn. To our surprise, we were able to detect expression in the border cells (Figure 4A) and the stress fibers (Figure 4B) of the epithelial follicle cells in the egg chamber, which are obviously not muscle cells. To determine which isoform the antibody was detecting, we used egg chamber lysates for Western analysis. The antibody detected a protein sized ~35 kDa. The annotated sizes for Tm1-L, Tm1-A, and Tm1-I are 32.5 kDa, 29.3 kDa, and 48 kDa, respectively. Isoforms A and L share many exons in common whereas I shares only one small exon with the other. We tested whether the antibody could recognize purified Tm1-A or Tm1-I proteins. Neither of the proteins was detected when probed with the monoclonal antibody, suggesting that the antibody detects isoform L (Figure 4C).

We next tested whether the antibody could recognize the Tm1-L isoform expressed in S2 R+ cells. HA-tagged Tm1-L under UAS promoter was induced with *actin*-Gal4. Upon induction, HA-tagged Tm1-L was expressed in the cytoplasm of the S2 R+ cells and was detected by an HA antibody. The monoclonal antibody also recognized the expressed protein, which colocalized with the HA expression. The monoclonal

antibody did not recognize the S2 R+ cells that were transfected with HA-Tm1-A or HA-Tm1-I (Figure 5A-C). Egg chambers from a transgenic fly line expressing HA-Tm1-L were also tested. The subset of follicle cells that expressed HA-Tm1-L, and thus over-expressed Tm1-L, stained brightly with the HA antibody and the monoclonal Tm antibody, while basal levels of endogenous Tm1-L were stained with the Tm-L antibody but not anti-HA (Figure 5D). These results indicate that the antibody is recognizing Tm1-L. Specifically, the antibody is detecting the epitope that is unique to Tm1-L, since it did not recognize either Tm1-A or Tm-I. 32 amino acids of Tm1-L in the N-terminus are unique to Tm1-L, while the rest of the isoforms overlaps with Tm1-A. We concluded that the epitope lies within these 32 amino acids, which are known to be common in all annotated muscle Tm isoforms (Hanke and Storti, 1988). As expected, the antibody detected muscle Tm isoform expressions in the muscle sheath enclosing the egg chamber (Figure 5E).

Since antibodies that could detect isoforms Tm1-A and Tm1-I were not commercially available, we set out to produce them using rabbits. As a first attempt, polyclonal antibodies were generated using peptide sequences specific for Tm1-A or Tm1-I. The antibodies successfully detected the purified Tm1-A and Tm1-I in Western (Data not shown). However, the antibodies were not able to detect any proteins in the egg chambers. This suggested that the peptide sequences used to generate antibodies were not exposed and that these short peptides were not sufficient as antigens.

As our second attempt, polyclonal Tm1-A and Tm1-I antibodies were generated using purified full-length proteins. When we tested the antibodies using immunohistochemistry with egg chambers, the Tm1-A antibody stained all follicle cells,

including the border cells and the epithelial follicle cells (Figure 6A). The Tm1-I antibody showed that Tm1-I is also expressed in the border cells and follicle cells, but is also slightly expressed in the germ line cells, including the cytoplasm of the nurse cells and the oocyte, especially near the pole plasm (Figure 6B, arrow).

The antibodies' cross-reactivity was determined using purified proteins on Western. The Tm1-A antibody only detected the Tm1-A protein and the Tm1-I antibody only detected the Tm1-I protein (Figure 7A). Next, we overexpressed either Tm1-A or Tm1-I in a subset of follicle cells to see if the antibodies can detect the proteins. Tm1-A antibody detected the elevated level of Tm-A protein but not overexpressed Tm1-I protein (Figure 7B), and Tm1-I overexpression was detected only with the Tm1-I antibody, not the Tm1-A antibody (Figure 7C)

Tm1 is highly expressed on basal F-actin stress fibers of the epithelial follicle cells.

Highly dense actin fibers are observed in the basal layer of the follicle cells when stained with fluorescently labeled Phalloidin. In order to see if Tm1 functions in regulating these structures, we first tested if we could detect Tm1 expression in the follicle cells using isoform-specific antibodies. We observed that all Tm1 isoforms colocalized with the phalloidin staining of actin filaments (Figure 8). Interestingly, the Tm1 filaments seemed more abundant than the actin filaments. While both Tm1-A and Tm1-L localized in the fibers and at the cortex of each cell Tm1-I only decorated the actin bundles. These localization patterns seem to evolve during egg chamber. However, details regarding stage-dependent isoform localization on actin filaments remain to be explored.

Tm1 is required for border cell migration

A dense actin network is observed in the lamellipodia of the leading cell in the border cell cluster during migration. Many actin binding proteins have been identified to regulate actin dynamics during border cell migration. In order to see whether tropomyosin, a well-known actin binding protein, is also involved in border cell migration, several Tm1 mutant alleles were obtained from Bloomington Drosophila Stock Center (BDSC) and Fly Trap (Yale). Tm1 homozygous mutant border cell clones were generated using MARCM (mosaic analysis with a repressible cell marker) (Wu and Luo, 2006), and the border cell migration index was counted (Figure 9). In both the $Tm1^{su(flw)4}$ and $Tm1^{zcl0722}$ lines, 80% of the stage 10 egg chambers containing homozygous mutant clusters showed a border cell migration defect (Figure 9B,C). In $Tm1^{pz2299}$ null mutant border cells, 60% of the stage 10 egg chambers had migration defect (Figure 9D,E)

Since we did not know the nature of the mutations in these lines, we decided to generate a Tm1 null line ($Tm1^{null}$) by utilizing a homologous recombination technique. We replaced the common exon (135 bp), which has the highest homology to the mammalian Tropomyosin, with the w+ gene (Figure 10A). Immunohistochemistry using antibodies that detect Tm1-L, Tm1-A and Tm1-I showed that these proteins were either lost or highly reduced in the homozygous null follicle cells (Figure 10B-D) including homozygous null border cells (Figure 11A-C), confirming that knocking out the common exon leads to null phenotypes. In order to determine whether $Tm1^{null}$ border cells show any migration defect, homozygous null border cells were generated to score migration

index. 70% of stage 10 egg chambers with Tm null border cells showed impaired migration (Figure 11D). In addition, during our antibody analysis, we identified that the mutant allele $Tm1^{zcl0722}$ showed absence of all three Tm1 isoforms, suggesting that this line may also serve as a null allele. Moreover, the mutant phenotypes of $Tm1^{zcl0722}$ were comparable to that of $Tm1^{null}$.

Three Tm1 isoforms have non-redundant functions in border cell migration

We have identified that three different isoforms are expressed in border cells of the egg chamber. Absence of all three isoforms together resulted in a border cell migration defect. We next wanted to test whether each of these isoforms is required individually for border cell migration. In order to do so, we needed isoform specific mutant alleles and RNAi lines that targeted each specific isoform.

Previously, $Tm1^{pz02299}$ was generated by P-element insertion (Tetzlaff et al., 1996). The Tm1-A isoform is disrupted by a P-element insertion in the 20th amino acid of the first exon. The homozygous larvae had a defect in head morphogenesis and soon die during first instar stage. Another study showed that $Tm1^{pz02299}$ functions in regulating dendrite size during neuronal development (Li and Gao, 2003). Specifically, mutant $Tm1^{pz02299}$ flies showed increased dendritic field sizes of neurons in embryos.

We found that $Tm1^{pz2299}$ homozygous mutant border cells gave 60% migration defect, and the migration defect was rescued by re-expressing the Tm1-A isoform whereas, Tm1-I was not able to rescue the defect (Figure 12A). These results confirm that $Tm1^{pz2299}$ affects Tm1-A but not I. Overexpression of UAS-RFP-Tm1-A in wild type

did not cause any detectable phenotype in border cells or in follicle cells. Reduced level of Tm1-A protein was observed with the Tm1-A antibody in $Tm1^{pz2299}$ homozygous mutant cells (Figure 12B). The residual antibody expression that is detected by the Tm1-A antibody in the Tm1-A mutant cells is very likely the expression of Tm1-L, which shares many exons in common with A. The Tm1-A antibody is therefore termed Tm1-A/L antibody since it recognizes both isoforms. Tm1-L and Tm1-I expression were unchanged in $Tm1^{pz02299}$ homozygous mutant cells, confirming its specific effect on A isoform.

We generated a UAS-Tm-A ^{RNAi} line and crossed with follicle cell driver to specifically knock down Tm1-A. However Tm1-A expression was only slightly reduced compared to the wild type, as seen with the Tm1-A/L antibody. The level of reduction was far less compared to the $Tm1^{pz02299}$ homozygous mutant follicle cell staining (Figure 12C), and the Tm1-A-RNAi expressing border cells did not cause a border cell migration defect.

$Tm1^{su(flw)4}$ flies were generated by Vereshchagina et al. by ethyl methanesulfonate (EMS) mutagenesis (Vereshchagina et al., 2004). The flies were isolated as a suppressor for a mutant protein phosphatase 1(PP1), a regulator of non-muscle myosin, and were shown to fail to complement $Tm1^{02299}$. During our study, we found that $Tm1^{su(flw)4}$ flies did not complement the $Tm1^{zcl0722}$ or the $Tm1^{null}$. Contrary to previous report, however, the ems mutant flies partially complimented $Tm1^{02299}$ (6.5% of the viable progeny were $Tm1^{02299}$ /$Tm1^{su(flw)4}$). However, all the viable $Tm1^{02299}$ /$Tm1^{su(flw)}$4 flies had a smaller wing phenotype, indicating incomplete complementation. Therefore $Tm1^{su(flw)4}$ appears to be a hypomorphic mutation.

We then performed antibody analysis to determine which of the Tm1 isoforms were affected by the $Tm1^{su(flw)4}$ allele. Interestingly, Tm1-I was reduced in $Tm1^{su(flw)4}$ homozygous mutant cells (Figure 13A), whereas Tm1-L and Tm1-A levels were unchanged. However, the localization of Tm1-L and Tm1-A proteins was altered, such that the proteins were abundant in the apical layer of the follicle cells compared to their normal basal localization (Figure 13B,C). These results led us to conclude that the $Tm1^{su(flw)4}$ allele partially disrupted Tm1-I isoforms, which in turn affected the localization but not the abundance of Tm1-L and Tm1-A.

We used $Tm1^{su(flw)4}$ to analyze the affect of reduced Tm1-I in border cells. In more than 80% of stage 10 egg chambers containing homozygous mutant clusters, border cells either could not detach or stopped in the middle of their migration. The migration defect was rescued by re-expression of Tm1-I, but not Tm1-A (Figure 14A). To confirm Tm-I isoform function, Tm1-I was knocked down using either *slbo*-Gal4 or *c306*-Gal4 drivers and UAS-Tm1-I^{RNAi} that specifically targeted the Tm1-I isoform under UAS promoter. Tm1-I was reduced in Tm1-I RNAi expressing cells detected by Tm-I antibody (Figure 14B). The reduction of Tm1-I in the border cells caused migration defect of 30~50%.

A UAS-Tm1-L ^{RNAi} line was generated using a hairpin construct that specifically targeted the Tm1-L isoform, but not Tm1-A or Tm1-I. The Tm1-L isoform was knocked down using either *slbo*-Gal4 or *c306*-Gal4 drivers. Using the Tm1-L antibody, we confirmed that Tm1-L was effectively knocked down in Gal4 expressing cells (Figure 15A). However, Tm1-L-negative border cells did not show any migration defect compared to the control (Figure 15B). We concluded that Tm1-L is not required for

border cell migration. Taken together, we found that isoforms Tm1-A and Tm1-I are required for border cell migration and although Tm1-L isoform is highly expressed in border cells, it is not involved in regulating their migration. Thus Tm1-A and Tm1-I have non-redundant functions in border cell migration.

Tm1 functions to regulate actin filaments in the basal layer of the epithelial follicle cells.

To determine if Tm1 is a regulator of actin filaments in the epithelial follicle cells, we crossed the $Tm1^{null}$ line with MARCM flies to generate homozygous null Tm1 follicle cells. The null cells indeed lacked Tm1-L, Tm1-A and Tm1-I proteins. When compared to neighboring wild type cells, we observed around a 40% reduction of phalloidin staining of actin fibers in homozygous null follicle cells (Figure 16A)**.**

Cytoskeletal tropomyosin is known to regulate myosin binding to actin filaments *in vitro* (Barua et al., 2014; Bryce et al., 2003; Tojkander et al., 2011). Previous studies show that myosin II regulates acto-myosin contractility in actin bundles of the basal layer of epithelial follicle cells (He et al., 2010). Since we observed reduction of actin filaments in $Tm1^{null}$ cells, we wanted to see if there was any change to the myosin localization on the stress fibers. Using the red fluorescent protein mcherry fused to a myosin regulatory light chain called Spaghetti squash (Sqh-mcherry), we were able to observe myosin accumulation in Tm^{null} homozygous mutant cells. Surprisingly, the level of myosin II activity observed by sqh-mcherry intensity was rather increased (Figure 16B). The level of increase varied from 30% to an almost 2 fold increase of myosin II

activity, detected by sqh-mcherry level compared to that of neighboring wild type cells (Figure 16C).

Three Tm1 isoforms function non-redundantly to regulate actin filaments in the epithelial basal layer

We then tested for isoform specific functions during stress fiber regulation in the epithelial follicle cells. In order to determine whether Tm1-A functions in regulating stress fibers, we made homozygous $Tm1^{pz2299}$ follicle cells using the MARCM technique. Detected by phalloidin staining, Tm1-A mutant follicle cells showed normal stress fiber labeling that was comparable to wild type (Figure 17A). The same phenotype was seen using UAS-Tm1-A^{RNAi} (Figure 17B).

UAS-Tm1-L^{RNAi} was expressed in a subset of follicle cells to test for its involvement in actin filament regulation. Confirmed by Tm1-L antibody staining, Tm1-L was undetectable in follicle cells expressing the RNAi (Figure 17C). The phalloidin staining was not altered in Tm1-L-negative cells, showing comparable level to the neighboring wild type cells (Figure 17D). However, it is not clear whether the Myosin II accumulation on the stress fibers remains the same in these Tm1-A or Tm1-I mutant cells. It is possible that although the phenotype in fixed tissue is not disturbed, the mutation may have affected the contractile function of the actin bundles, a hypothesis we are currently testing.

Overexpressing Tm1-I did not alter the phalloidin staining of the stress fibers. However, when Tm1-I was reduced using RNAi, the phalloidin staining was reduced by

40%. UAS-Tm1-I^{RNAi}-expressing follicle cells (Figure 18A) also showed reduction in myosin light chain accumulation detected by sqh-mcherry expression (Figure 18B). Tm1$^{su(flw)4}$ homozygous mutant follicle cells were observed for actin bundles to see if there was any defect in the actin cytoskeleton. The homozygous Tm1$^{su(flw)}$4 follicle cells had 40% lower phalloidin staining in their stress fibers compared to the neighboring wild type cells (Figure 18C). Furthermore, we found that reduction of Tm1-I in the follicle cells caused up to 40% reduction in myosin accumulation compared to the control (Figure 18D). In addition to the reduction of the basal actin and myosin light chain levels in the homozygous mutant cells, we also observed reduced follicle cell diameter. The difference of cell size is more pronounced when the mutant clone is small (Figure 19).

Taken together**,** neither Tm1-L nor Tm1-A alone is required for actin fiber regulation while Tm1-I functions to regulate actin bundles. Without Tm1-I, there is reduction of actin filaments and impairment of its contractile functions suggested by reduction of Myosin II expression. We propose that in this cellular context, Tm1-A and Tm1-I likely function redundantly because the phenotype of the Tm1 null allele, in which all isoforms are deleted, is distinguishable from the loss of Tm1-I alone. Isoform specific rescue experiments and double knockdowns are currently underway to test this hypothesis.

Tm1 isoforms interact with each other to regulate their function and expression

During the antibody analysis, we found that the Tm1-I antibody not only detected Tm1-I overexpression, but that it also showed slightly elevated level in the cells that had

exogenous Tm1-A protein (Figure 20A). A similar phenotype was seen using RNAi knockdowns. When Tm1-A was knocked down using UAS-Tm1-A^{RNAi}, Tm1-I expression detected by the Tm1-I antibody was also reduced (Figure 20B). Since UAS-Tm1-A^{RNAi} was made only to target the Tm1-A isoform, it is not possible that Tm1-I was also knocked down. In order to rule out the possibility of the antibodies recognizing each other, we performed Western with purified proteins. The Western results suggested that there is no cross-reactivity between the antibodies. These results suggest that Tm1-A might play a role in regulating Tm1-I. It is possible that Tm1-A and Tm1-I co-assemble onto the actin stress fibers. In addition to these possible interactions, in Tm1-A mutant follicle cells, Tm1-L failed to localize to the cell membrane, suggesting that Tm1-A and Tm1-L may also interact, suggesting that these isoforms co-assemble there (Figure 20C). Taken together, Tm1 isoforms interact together to regulate their function and expression, to further regulate actin dynamics.

Discussion

Tropomyosin (Tm) was first identified as a muscle regulator in 1946. Since then, the protein has been extensively studied, elucidating its complex function and involvement in muscle regulation. However, tropomyosin is also expressed in non-muscles cells, where it regulates the actin cytoskeleton. While less is known regarding non-muscle Tm function, emerging evidence shows that different Tm isoforms promote the assembly, structure, stability and contractile function of diverse types of actin filaments, which influences cellular activities such as cell motility, cell adhesion, and cytoskeletal architecture.

We have carried out a systematic analysis of the three Tm isoforms that we detected in follicle cells in the Drosophila ovary, although we cannot exclude the possibility that other isoforms are expressed at levels that were not detected by the mRNA tagging experiment. While this remains a possibility, we are confident that our $Tm1^{null}$ line is a true null and that it's mutant phenotype is a representative Tm1 mutant.

Several lines of evidence suggest that the ems induced mutation in the $Tm1^{su(flw)4}$ allele reduces expression of the Tm1-I isoform: Tm1-I re-expression, but not Tm1-A, rescued the border cell migration defect phenotype in $Tm1^{su(flw)4}$ clones. In addition, Tm1-I RNAi phenocopied the $Tm1^{su(flw)4}$ mutant phenotype, in both border cells and epithelial follicle cells. We note that Tm1-L and Tm1-A proteins were mis-localized in $Tm1^{su(flw)4}$ mutant cells, suggesting that Tm1-I is required to recruit Tm1-L and Tm1-A to the basal actin stress fibers. Thus, the phenotype may be due to a combinatorial effect of reduction of Tm1-I and mis-localization of Tm1-L and Tm1-A. Consistent with this interpretation, neither $Tm1^{su(flw)4}$ nor Tm1-I RNAi showed complete elimination of Tm1-I

antibody staining yet $Tm1^{su(flw)4}$ caused the most drastic phenotype, seemingly even stronger than the null.

Tm1-L is expressed in non-muscle cells

In one of the earlier papers that investigated *Drosophila* Tm1, Tm1-L was annotated as a muscle-specific isoform (Hanke and Storti, 1988). This categorization was due the fact that Tm1-L relies on a promoter that transcribes all other muscle specific Tm1 isoforms. Thus, Tm1-L includes two exons that are common in all muscle isoforms. The rest of the protein sequence overlaps with the Tm1-A isoform. Fortunately, we obtained a commercial antibody that could recognize Tm1-L. To our surprise, the Tm1-L isoform was nicely expressed in the border cells and the follicle cells. Also, Tm1-L specifically decorated the stress fibers in the basal layer of the epithelial follicle cells. Since the epitope lies in what was known as a muscle specific exon, we tested the antibody in the muscle sheath that encloses the egg chambers. As expected, the antibody showed nicely decorated sarcomeric patterning of Tm in the muscle sheath. However, since all Tm1 muscle forms have a common epitope, it is not clear which muscle isoform(s) the antibody was detecting.

Our results indicate that Tm1-L is expressed in non-muscle cells. However, when we knock down Tm1-L in border cells and in outer follicle cells, we did not see any significant mutant phenotype. It is possible that the Tm1-L isoform is not involved in border cell migration or actin bundle regulation. However, it is also possible that Tm-A and Tm-L function redundantly, as Tm1-A and Tm1-L are 91% identical in amino acid

sequence. Due to this fact, we might not have observed border cell migration defect when only Tm1-L was knocked down. To test this possibility, we could reduce the level of both Tm1-A and Tm1-L together to see if this results in any mutant phenotype. The double knockdown flies will be useful to examine the effect of these two proteins in regulating the stress fibers in the epithelial follicle cells. Alternatively Tm-L may function at an earlier or later stage of development. Another possibility is that Tm1-L's sole function is to regulate muscle related actin filaments. It would be interesting to test Tm1-L's role in regulating muscle fibers such as those in the muscle sheath, a muscle structure enclosing the egg chamber.

Tm1-I may play a role in *oskar* mRNA localization

All Tm1 isoforms identified in the egg chamber were expressed in the follicle cells. Tm1-I showed unique expression in germline cells. Specifically, Tm1-I showed sharp localization at the posterior of the oocyte (Figure 5B, arrow). Germ cell expression of the Tm1 isoform is interesting, since previous studies reported that Tm1 mutants showed impaired *oskar* mRNA localization. (Erdelyi et al., 1995; Tetzlaff et al., 1996; Zimyanin et al., 2008). Oskar mRNA is required for posterior pole plasm assembly, and mis-localization causes impaired development of the abdomen and germ cells. During egg chamber stages 8 to 10, *oskar* mRNA moves toward the posterior of the oocyte, where it is then translated to nucleate the polar granules (Kim-Ha et al., 1991). Involvement of Tm1 in *oskar* mRNA localization has been a puzzle because mRNA localization was known to solely require microtubules and microtubule motors such as kinesin. The *oskar*

localization was abolished when the egg chambers were treated with a microtubule destabilizing drug such as colchicine (Clark et al., 1994). After involvement of Tm1 was observed, some reports suggested that *oskar* is delivered to the microtubules via an actin based mechanism at the anterior of the oocyte for subsequent transport to the posterior. However, there is no significant evidence to support this idea. The observation that Tm1-I localizes to the posterior of the oocyte suggests that it might be required to anchor *oskar* mRNA there. In order to determine which if any Tm1 isoforms are required for oskar mRNA transport, we will determine which isoforms are affected in the mutant alleles Tm1eg and Tm1gs, which cause *oskar* mRNA mis-localization. These alleles were generated by p-element insertion, but it is not known which isoform(s) was disrupted. It would be interesting to test whether the level of Tm1-I is reduced in these flies and if Tm1-I plays an active role in *oskar* localization and germline specification. Since Tm1 binds to actin filaments and regulates actin cytoskeleton, it may be possible that actin filaments are involved in mRNA transportation. However, studies show that egg chambers treated with the actin targeting drug Latrunculin A show normal transportation of osk mRNP (Zimyanin et al., 2008), indicating that Tm1 may be directly involved in mRNA transportation, rather than as an actin regulator. It is possible that Tm1-I forms a higher order polymer that forms a complex with osk mRNP, which are together required for normal *oskar* mRNA localization via microtubules. Tm1-I has a unique structure, with a long N-terminal tail that is composed of a disordered amino acid sequence, a partial coiled coil section in the middle, and a C-terminus with an additional random amino acid stretch. It is possible that this long tail is involved in forming a multimer, as has been shown recently for RNA and DNA binding proteins (Han et al., 2012; Kato et

al., 2012). This unique protein structure suggests that Tm1-I may have a distinctive function to serve an important cellular activity.

Tropomyosin impacts actin dynamics

Tropomyosin in non-muscle cells has been yet characterized as an actin filament stabilizer. However, recent findings suggest that Tm can either increase or decrease actin filament stability depending on which tropomyosin isoform is associated (Creed et al., 2008)

Involvement of Tm1 in border cell migration may be straightforward. Absence of Tm1 disturbs the stability of actin filaments. And reduction in actin stability inhibits migration. We found that when EGFP-actin was overexpressed in the background of heterozygous Tm1 mutants, the protrusions of the border cells could not retract, but rather showed constant protrusion, forming a long and thin extension (Kim et al., 2011). This phenotype resembled non-muscle myosin II in border cell migration (Fulga and Rorth, 2002). However, it is not yet clear whether this defect is a direct effect of loss of actin stability or if it is indirect. Non-muscle tropomyosin *in vitro* antagonizes the actin filament severing activity of cofilin (Ono and Ono, 2002). Since cofilin also regulates border cell migration (Chen et al., 2001; Zhang et al., 2011), cofilin and Tm1 may show antagonizing functions in border cells.

In the outer follicle cells, myosin normally accumulates on and dissociates from the basal stress fibers periodically (He et al., 2010).. Our results suggest that Tm1 plays more than one key role in this process. In follicle cells mutant for $Tm1^{su(flw)4}$, which

reduced the level of Tm1-I and mis-localized Tm1-A and Tm1-L, the level of phalloidin staining of actin fibers and myosin light chain accumulation were reduced. However, when all isoforms were eliminated in the null allele, an increase in myosin light chain level resulted despite reduced levels of phalloidin staining. This shows that in the null myosin cannot dissociate from the filaments suggesting that one or more isoforms of Tm normally assist in the dissociation of myosin. It is possible that while wild type cells have oscillating myosin activity, the Tm1 mutant cells have myosin II locked onto the actin fibers which hinders contractility and further actin regulation. Live-imaging will help us to understand how myosin II is regulated in these mutants. This suggests that perhaps the oscillating function of myosin II is more important for actin filament stabilization

Here we have described a systematic analysis of the expression and function of Tm1 isoforms in the fruit fly ovary. We found that Tm1 is a key regulator of the collective cell migration of border cells and plays an important role in stress fiber formation and function in epithelial follicle cells. Interestingly, three different tropomyosin isoforms function together to coordinate distinct actin dynamics in each cell type. During our study, we generated isoform-specific antibodies, isoform-specific RNAi lines, and isoform-specific mutant lines that will continue to be invaluable in deciphering the functions of Tm1 and its interacting proteins in these cell types and will provide tools for other investigators to study the roles of Tm1 isoforms in other tissues and processes for years to come

Material and Methods

Drosophila Strains and Genetics

$Tm1^{zcl0722}$ was obtained from Flytrap. Both $Tm1^{pz2299}$ and $Tm1^{su(flw)4}$ lines were ordered from BDRC. In order to make homozygous mutant cells, these lines were recombined with FRT 82B. hsp70-*FLP*,*tub*-Gal4,UAS-GFP-nls; FRT82B, *tub*-Gal80 (MARCM : mosaic analysis with a repressible cell marker) was crossed with FRT 82B;Tm1 mutant lines to generate positive GFP mutant clones. Heat shock was performed either using 3rd instar larvae or 2 day old female adults. Large homozygous mutant clones were generated when 3rd instar larvae was heat shocked for 2hrs at 37°C. The vials were kept at 25°C until the female flies enclosed. Then the flies were transferred into a new vial with ample food and kept in 29°C overnight before dissection. Adult heat shock was performed with 2 or 3 day old female flies. Either three heat shocks for two days or two heat shocks for three days at 37°C were used to generate mutant clones. The heat shocked flies were kept in 25°C and dissected 5~7 days after the first heat shock.

hsp70-FLP; Ay17bGal4, UAS-moesin-GFP or hsp70-FLP; Ay17bGal4,UAS-RFPnls was used to generate Flp-out clones. Heat shock was performed with two day old adult females, twice a day for two days and the flies were kept in 29°C until ovaries were dissected out 2~3 days later.

sqh::sqh-mcherry flies were used to detect myosin accumulation. Follicle cell drivers *Cy2*-Gal4 and *tub*-Gal4 were used for exogenous expression of Tm1 isoforms in follicle cells.

Immunohistochemistry and Imaging

Ovaries were dissected in Schneider's medium (GIBCO) supplemented with 10% FBS (Sigma) and fixed for 15 minutes in 4% paraformaldehyde. After three 15 minute washes with PBT (1x PBS, 0.1% Triton x-100) the egg chambers were blocked with PBT block (1x PBT, 5% goat serum) 2 hours at room temperature or overnight at 4°C. Primary antibodies were treated overnight at 4°C followed by secondary antibody incubation at room temperature for 1 hour. Primary antibodies rat anti-Tm (1:5000, abcam), Tm-A (1:1000), Tm-I (1:800). Alexa Fluor conjugated goat anti-rabbit or anti-rat IgG antibodies were used as secondary antibodies (Molecular Probes). Alexa phalloidins, 488 or 568 (1:200) were used to stain the actin filaments. DAPI (1:10000) was used to mark the nucleus. After three 15 minute washes, the samples were mounted with Vectashield (Vector Laboratories). Zeiss 780 was used for imaging most images.

Generating Tm1-A and Tm1-I antibodies

Two peptide sequences below were used to generate polyclonal antibodies in rabbits (Genscript).

Tm-I antigen sequence: CKSSGKKERSKRSNP

Tm-A antigen sequence: CNLKSLEVSEEKATQ

For polyclonal antibody generation using full-length proteins as antigens, two full length Tm1-I and Tm1-A constructs were made. Tm1-I was amplified using specific primers and Drosophila EST LD11194 as a template. LD37158 was used for Tm1-A amplification. Each amplified sequence was cloned into pET28-a vector (clonetech). The plasmids were transformed into BL21 cells and the protein was induced using 0.5mM IPTG. The His tagged proteins were purified using Ni-NTA His Bind Purification kit (Novagen) and eluted with 100mM and 250mM imidazole. Total of 5mg of each protein was purified and concentrated and sent out to Antibodes, Inc for antibody generation. The protein antigens were injected into rabbits following general antibody production procedure.

mRNA tagging method to isolate follicle cell specific mRNA

P[*UAS-hPABP-FLAG*] (BL#9419) was crossed with Slbo-Gal4 or C306-Gal4 driver to drive FLAG tagged poly-A binding protein expression in border cell specific cells. The mRNA tagging method was adapted from a previous paper (Yang et al., 2005). Briefly, 400 ovaries were dissected and fixed with 1 ml of PBS containing 1% formaldehyde and 0.5% NP-40 for 30 minutes at 4°C. After fixation, 140µl of 2M glycine was added and incubated for additional 5 minutes at 4°C. The ovaries were washed three times with 1x PBS and then homogenized in 0.8ml of homogenization buffer (HB : 150mM NaCl,

50mM HEPES buffer pH 7.6, 1mM EGTA, 15mM EDTA, 10% glycerol) Immediately before homogenization, 50U/ml SUPERase-In (Ambion) was added and 1 tablet of Protease Inhibitor Cocktail (Roche) was added per 10ml of HB. The ovaries were sonicated for 1min using 30% intensity using Fisher Sonic Dismembrator, Model 500. The supernatant was collected after centrifuging for 10 minutes at 13,000 × g and added to 100µl of Anti-FLAG-M2 affinity agarose beads (Sigma-Aldrich) that were equilibrated with HB. The supernatant and bead mix were incubated at 4°C for 2 hours with gentle rotation. The beads were washed with HB for four times and the mRNA was eluted by incubating the beads with the elute buffer (50mM Tris-HCl pH 7.0, 10mM EDTA, 1.3% SDS, 50U/ml SUPERase-IN) at 65°C for 30 minutes.

RT-PCR amplification of Tm1 isoforms

mRNA from the elute was isolated using Trizol and its protocol (ambion). The isolated mRNA was reverse transcribed to cDNA using the Superscript III following its protocol (Invitrogen).

Muscle (Includes Tm-N, Tm-O, Tm-J) : Tm1MF & Tm1MR

Tm1-C : TmRC1 (F) & Tm1-2 (R)

Tm1-A: TmRA6F & TmRA2 (R)

Tm1-I: TmRI6 (F) & TmRI5 (R)

Tm1-L: TmRA6-F & TmRL-R

Tm1-Q : TmRA1 (F)& TmPQ1 (R)

Tm1-P: Tm1M-F & TmRP-R

Tm1-F: TmAll1-F & TmRF-R

Tm1-K: TmAll1-F & TmRK-R

TmRA1: 5’ GCATATTCGCCTGCCAGTTT 3’

TmRC1: 5’ CAGAAAAGCCAGCAGCAGCC 3’

TmRI6: 5’ GATAAGGCGAAGGAGAAGTC 3’

TmRI5: 5’ GGCTGTGCATGATCTAGGTC 3’

TmRA2: 5’ CGCTAGCTGCCAGTCAACCG 3’

Tm1-2: 5’ CGGTGCATTTCTTGCTGATC 3’

TmRA6F: 5’ AAAGCGCTTGAGAATCGCA 3’

TmAll1-F: 5’ AACGTCGCATCCAGTTGCT 3’

TmRL-R: 5’ GCAATTGCAGCAGCATGGTA 3’

TmRP-R: 5’ GAATTTGTCGCAGCATTGCG 3’

TmRF-R: 5’ GACAGCAACAACATATGCTC 3’

TmRK-R: 5’ TGCTTCAGCTGGAGGAGCTT 3’

TmPQ1-R: 5’ GGACTCCATTTGTCTTCATC 3’

Generating transgenic flies expressing Tm1-A and Tm1-L RNAi hairpins

Hairpin sequences below was selected and cloned into VALIUM20 vector by TRiP facility (Havard). The hairpin targets the first exon of Tm1-A and Tm1-L, respectively.

Tm1-A hairpin sequence AAGAAGATGCGCCAGACCAAA (sense)

TTTGGTCTGGCGCATCTTCTT (antisense)

Tm1-L hairpin sequence GCAAGCGATGAAAGTCGACAA (sense)

TTGTCGACTTTCATCGCTTGC (antisense)

The amplified plasmid was injected into y v ; nanos-integrase; attP40 (2nd chromosome) or y v ; nanos-integrase;attP2 (3rd chromosome) by Rainbow transgenics.

Generating homologous recombinant line using ends out targeting technique

In order to generate $Tm1^{null}$, we took advantage of ends out targeting method (Gong and Golic, 2003). Gene region that is common in all isoform (135bp) was targeted for deletion.

Left arm primers – Forward: 5' GTTGGCCTTCTAGCTTTCTG 3'

Reverse: 5' GACAAACGTTCGATGGACGA 3'

Right arm primers – Forward: 5' AGTACCACGTTACCATCTA 3'

Reverse: 5' GGTCCCAGTTATGGATTCCA 3'

The left arm and right arm was amplified using above primers and w1118 genomic DNA as the template. The two ~3kb fragments were inserted into pW35 vector using Infusion cloning (Clontech) and was verified by sequencing. The cloned plasmid was amplified was injected into W1118 flies (Bestgene). The flies were crossed to hs-flp hs-ISceI /CyO

and heat shocked to excise and linearize the common exon targeting insert. Successful deletion/replacement with w+ was confirmed by PCR.

Generating transgenic lines

Tm1-I was amplified using specific primers and Drosophila EST LD11194 as a template. LD37158 was used for Tm1-A amplification. Since cDNA for Tm1-L did not exist, two PCR fragments amplified from RE08101 and LD37158 were combined to make full length Tm-L. The amplified sequences were cloned into HA-UASt vector for N terminal HA tag expression or EGFP-UASt vector for N terminal EGFP tagged protein. Some of the expression vectors were made by utilizing available Gateway vectors and its cloning system (Invitrogen). Cloned plasmid was verified by sequencing and sent to Bestgene for transgenic fly generation. Collection of UAS-EGFP-Tm1-A, UAS-EGFP-Tm1-I, UAS-EGFP-Tm1-L, UAS-Tm1-A-RFP, UAS-Tm1-I-EGFP, UAS-HA-Tm1-A, UAS-HA-Tm1-I, and UAS-HA-Tm1-L was made for this project.

S2 R+ expression of Tropomyosin isoforms

S2 R+ cells were plated onto 6 well plate with cover glass in each well. Different HA-tagged Tm1 constructs under UAS promoter along with *actin*-Gal4 were transfected into S2 R+ cells induce expression using Effectene (Qiagen). The cells were incubated in RT for 48 hours before they were processed for immunohistochemistry. Briefly, 4% paraformaldehyde in PBS was used to fix for 10 minutes. After three washes using PBST

(1x PBS, 0.1% Triton-X100), the cells were incubated with mouse HA antibody (1:1000) and rat Tm-L antibody for 2 hours. Secondary antibodies conjugated with Alexa-568 (mouse) and Alexa-488 (rat) was in 1:400 dilutions. Vectashield was used to mount coverslips on slides for imaging.

References

Bach, C.T., Creed, S., Zhong, J., Mahmassani, M., Schevzov, G., Stehn, J., Cowell, L.N., Naumanen, P., Lappalainen, P., Gunning, P.W.*, et al.* (2009). Tropomyosin isoform expression regulates the transition of adhesions to determine cell speed and direction. Molecular and cellular biology *29*, 1506-1514.

Bailey, K. (1946). Tropomyosin: a new asymmetric protein component of muscle. Nature *157*, 368.

Barua, B., Nagy, A., Sellers, J.R., and Hitchcock-DeGregori, S.E. (2014). Regulation of nonmuscle myosin II by tropomyosin. Biochemistry *53*, 4015-4024.

Bautch, V.L., Storti, R.V., Mischke, D., and Pardue, M.L. (1982). Organization and expression of Drosophila tropomyosin genes. Journal of molecular biology *162*, 231-250.

Behrmann, E., Muller, M., Penczek, P.A., Mannherz, H.G., Manstein, D.J., and Raunser, S. (2012). Structure of the rigor actin-tropomyosin-myosin complex. Cell *150*, 327-338.

Blanchoin, L., Pollard, T.D., and Hitchcock-DeGregori, S.E. (2001). Inhibition of the Arp2/3 complex-nucleated actin polymerization and branch formation by tropomyosin. Current biology : CB *11*, 1300-1304.

Bryce, N.S., Schevzov, G., Ferguson, V., Percival, J.M., Lin, J.J., Matsumura, F., Bamburg, J.R., Jeffrey, P.L., Hardeman, E.C., Gunning, P.*, et al.* (2003). Specification of actin filament function and molecular composition by tropomyosin isoforms. Molecular biology of the cell *14*, 1002-1016.

Caldwell, B.J., Lucas, C., Kee, A.J., Gaus, K., Gunning, P.W., Hardeman, E.C., Yap, A.S., and Gomez, G.A. (2014). Tropomyosin isoforms support actomyosin biogenesis to generate contractile tension at the epithelial zonula adherens. Cytoskeleton *71*, 663-676.

Chen, J., Godt, D., Gunsalus, K., Kiss, I., Goldberg, M., and Laski, F.A. (2001). Cofilin/ADF is required for cell motility during Drosophila ovary development and oogenesis. Nature cell biology *3*, 204-209.

Clark, I., Giniger, E., Ruohola-Baker, H., Jan, L.Y., and Jan, Y.N. (1994). Transient posterior localization of a kinesin fusion protein reflects anteroposterior polarity of the Drosophila oocyte. Current biology : CB *4*, 289-300.

Creed, S.J., Bryce, N., Naumanen, P., Weinberger, R., Lappalainen, P., Stehn, J., and Gunning, P. (2008). Tropomyosin isoforms define distinct microfilament populations with different drug susceptibility. European journal of cell biology *87*, 709-720.

Creed, S.J., Desouza, M., Bamburg, J.R., Gunning, P., and Stehn, J. (2011). Tropomyosin isoform 3 promotes the formation of filopodia by regulating the recruitment of actin-binding proteins to actin filaments. Experimental cell research *317*, 249-261.

Erdelyi, M., Michon, A.M., Guichet, A., Glotzer, J.B., and Ephrussi, A. (1995). Requirement for Drosophila cytoplasmic tropomyosin in oskar mRNA localization. Nature *377*, 524-527.

Fulga, T.A., and Rorth, P. (2002). Invasive cell migration is initiated by guided growth of long cellular extensions. Nature cell biology *4*, 715-719.

Gimona, M., Watakabe, A., and Helfman, D.M. (1995). Specificity of dimer formation in tropomyosins: influence of alternatively spliced exons on homodimer and heterodimer assembly. Proceedings of the National Academy of Sciences of the United States of America *92*, 9776-9780.

Gong, W.J., and Golic, K.G. (2003). Ends-out, or replacement, gene targeting in Drosophila. Proceedings of the National Academy of Sciences of the United States of America *100*, 2556-2561.

Gunning, P., Gordon, M., Wade, R., Gahlmann, R., Lin, C.S., and Hardeman, E. (1990). Differential control of tropomyosin mRNA levels during myogenesis suggests the existence of an isoform competition-autoregulatory compensation control mechanism. Developmental biology *138*, 443-453.

Gunning, P., O'Neill, G., and Hardeman, E. (2008). Tropomyosin-based regulation of the actin cytoskeleton in time and space. Physiological reviews *88*, 1-35.

Han, T.W., Kato, M., Xie, S., Wu, L.C., Mirzaei, H., Pei, J., Chen, M., Xie, Y., Allen, J., Xiao, G.*, et al.* (2012). Cell-free formation of RNA granules: bound RNAs identify features and components of cellular assemblies. Cell *149*, 768-779.

Hanke, P.D., and Storti, R.V. (1988). The Drosophila melanogaster tropomyosin II gene produces multiple proteins by use of alternative tissue-specific promoters and alternative splicing. Molecular and cellular biology *8*, 3591-3602.

He, L., Wang, X., Tang, H.L., and Montell, D.J. (2010). Tissue elongation requires oscillating contractions of a basal actomyosin network. Nature cell biology *12*, 1133-1142.

Hendricks, M., and Weintraub, H. (1981). Tropomyosin is decreased in transformed cells. Proceedings of the National Academy of Sciences of the United States of America *78*, 5633-5637.

Jang, W.I., Jo, Y.J., Kim, H.C., Jia, J.L., Namgoong, S., and Kim, N.H. (2014). Non-muscle tropomyosin (Tpm3) is crucial for asymmetric cell division and maintenance of cortical integrity in mouse oocytes. Cell cycle *13*, 2359-2369.

Kato, M., Han, T.W., Xie, S., Shi, K., Du, X., Wu, L.C., Mirzaei, H., Goldsmith, E.J., Longgood, J., Pei, J.*, et al.* (2012). Cell-free formation of RNA granules: low complexity sequence domains form dynamic fibers within hydrogels. Cell *149*, 753-767.

Kim, J.H., Cho, A., Yin, H., Schafer, D.A., Mouneimne, G., Simpson, K.J., Nguyen, K.V., Brugge, J.S., and Montell, D.J. (2011). Psidin, a conserved protein that regulates protrusion dynamics and cell migration. Genes & development *25*, 730-741.

Kim-Ha, J., Smith, J.L., and Macdonald, P.M. (1991). oskar mRNA is localized to the posterior pole of the Drosophila oocyte. Cell *66*, 23-35.

Kubo, E., Hasanova, N., Fatma, N., Sasaki, H., and Singh, D.P. (2013). Elevated tropomyosin expression is associated with epithelial-mesenchymal transition of lens epithelial cells. Journal of cellular and molecular medicine *17*, 212-221.

Li, W., and Gao, F.B. (2003). Actin filament-stabilizing protein tropomyosin regulates the size of dendritic fields. The Journal of neuroscience : the official journal of the Society for Neuroscience *23*, 6171-6175.

Miyado, K., Sato, M., and Taniguchi, S. (1997). Transformation-related expression of a low-molecular-mass tropomyosin isoform TM5/TM30nm in transformed rat fibroblastic cell lines. Journal of cancer research and clinical oncology *123*, 331-336.

Muthuchamy, M., Pajak, L., Howles, P., Doetschman, T., and Wieczorek, D.F. (1993). Developmental analysis of tropomyosin gene expression in embryonic stem cells and mouse embryos. Molecular and cellular biology *13*, 3311-3323.

Novy, R.E., Lin, J.L., Lin, C.S., and Lin, J.J. (1993). Human fibroblast tropomyosin isoforms: characterization of cDNA clones and analysis of tropomyosin isoform expression in human tissues and in normal and transformed cells. Cell motility and the cytoskeleton *25*, 267-281.

Ono, S., and Ono, K. (2002). Tropomyosin inhibits ADF/cofilin-dependent actin filament dynamics. The Journal of cell biology *156*, 1065-1076.

Schevzov, G., Bryce, N.S., Almonte-Baldonado, R., Joya, J., Lin, J.J., Hardeman, E., Weinberger, R., and Gunning, P. (2005). Specific features of neuronal size and shape are regulated by tropomyosin isoforms. Molecular biology of the cell *16*, 3425-3437.

Stehn, J.R., Haass, N.K., Bonello, T., Desouza, M., Kottyan, G., Treutlein, H., Zeng, J., Nascimento, P.R., Sequeira, V.B., Butler, T.L.*, et al.* (2013). A novel class of anticancer compounds targets the actin cytoskeleton in tumor cells. Cancer research *73*, 5169-5182.

Talbot, K., and MacLeod, A.R. (1983). Novel form of non-muscle tropomyosin in human fibroblasts. Journal of molecular biology *164*, 159-174.

Tetzlaff, M.T., Jackle, H., and Pankratz, M.J. (1996). Lack of Drosophila cytoskeletal tropomyosin affects head morphogenesis and the accumulation of oskar mRNA required for germ cell formation. The EMBO journal *15*, 1247-1254.

Tojkander, S., Gateva, G., Schevzov, G., Hotulainen, P., Naumanen, P., Martin, C., Gunning, P.W., and Lappalainen, P. (2011). A molecular pathway for myosin II recruitment to stress fibers. Current biology : CB *21*, 539-550.

Vereshchagina, N., Bennett, D., Szoor, B., Kirchner, J., Gross, S., Vissi, E., White-Cooper, H., and Alphey, L. (2004). The essential role of PP1beta in Drosophila is to regulate nonmuscle myosin. Molecular biology of the cell *15*, 4395-4405.

von der Ecken, J., Muller, M., Lehman, W., Manstein, D.J., Penczek, P.A., and Raunser, S. (2014). Structure of the F-actin--tropomyosin complex. Nature.

Weinberger, R.P., Henke, R.C., Tolhurst, O., Jeffrey, P.L., and Gunning, P. (1993). Induction of neuron-specific tropomyosin mRNAs by nerve growth factor is dependent on morphological differentiation. The Journal of cell biology *120*, 205-215.

Wu, J.S., and Luo, L. (2006). A protocol for mosaic analysis with a repressible cell marker (MARCM) in Drosophila. Nature protocols *1*, 2583-2589.

Yang, Z., Edenberg, H.J., and Davis, R.L. (2005). Isolation of mRNA from specific tissues of Drosophila by mRNA tagging. Nucleic acids research *33*, e148.

Zhang, L., Luo, J., Wan, P., Wu, J., Laski, F., and Chen, J. (2011). Regulation of cofilin phosphorylation and asymmetry in collective cell migration during morphogenesis. Development *138*, 455-464.

Zimyanin, V.L., Belaya, K., Pecreaux, J., Gilchrist, M.J., Clark, A., Davis, I., and St Johnston, D. (2008). In vivo imaging of oskar mRNA transport reveals the mechanism of posterior localization. Cell *134*, 843-853.

Table 1. List of available Tm1 reagents

Mutant allele	Isoform	Reference
$Tm1^{su(flw)4}$	Tm1-I	Vereshchagina et al., 2004
$Tm1^{zcl0722}$	Tm1-A, Tm1-I, Tm1-L	Fly Trap
$Tm1^{pz2299}$	Tm1-A	Tetzlaff et al., 1996
$Tm1^{null}$	Tm1-A, Tm1-I, Tm1-L	Cho et al. 2015
UAS-Tm1-A^{RNAi}	Tm1-A	Cho et al. 2015
UAS-Tm1-L^{RNAi}	Tm1-L	Cho et al. 2015
UAS-Tm1-I^{RNAi}	Tm1-I	VDRC
UAS-EGFP-Tm1-I (HA or RFP tag)	Tm1-I	Cho et al. 2015
UAS-EGFP-Tm1-A (HA or RFP tag)	Tm1-A	Cho et al. 2015
UAS-EGFP-Tm1-L (HA tag)	Tm1-L	Cho et al. 2015

Antibodies	Isoform (s)	From
Tm1-L	L	Abcam (MAC 141)
Tm1-A	A and L	Cho et al. 2015
Tm1-I	I	Cho et al. 2015

Figure 1. *Drosophila* Tm1 isoform composition

Drosophila Tm1 gene (boxed) encodes 17 different isoforms. Coding exons are labeled in different colors to indicate shared exons among isoforms. Tm1-C and Tm-I; Tm1-G, Tm1-M, Tm1-J, and Tm1-O have the same amino acid composition but differ in their 3' and 5' untranslated region (UTR). Among these isoforms, only Tm1-L, Tm1-A and Tm1-I are expressed in the egg chambers. Tm1-A and Tm1-L have very similar coding exon composition except that Tm1-L has extra 32 amino acid in the N-terminus (pink and green exons). However, Tm1-I has very different exon composition compared to Tm1-A or Tm-L. The only common exon (sky blue) among these three isoforms is the common exon among all isoforms.

Isoform composition adapted from fly base http://flybase.org/reports/FBgn0003721.html

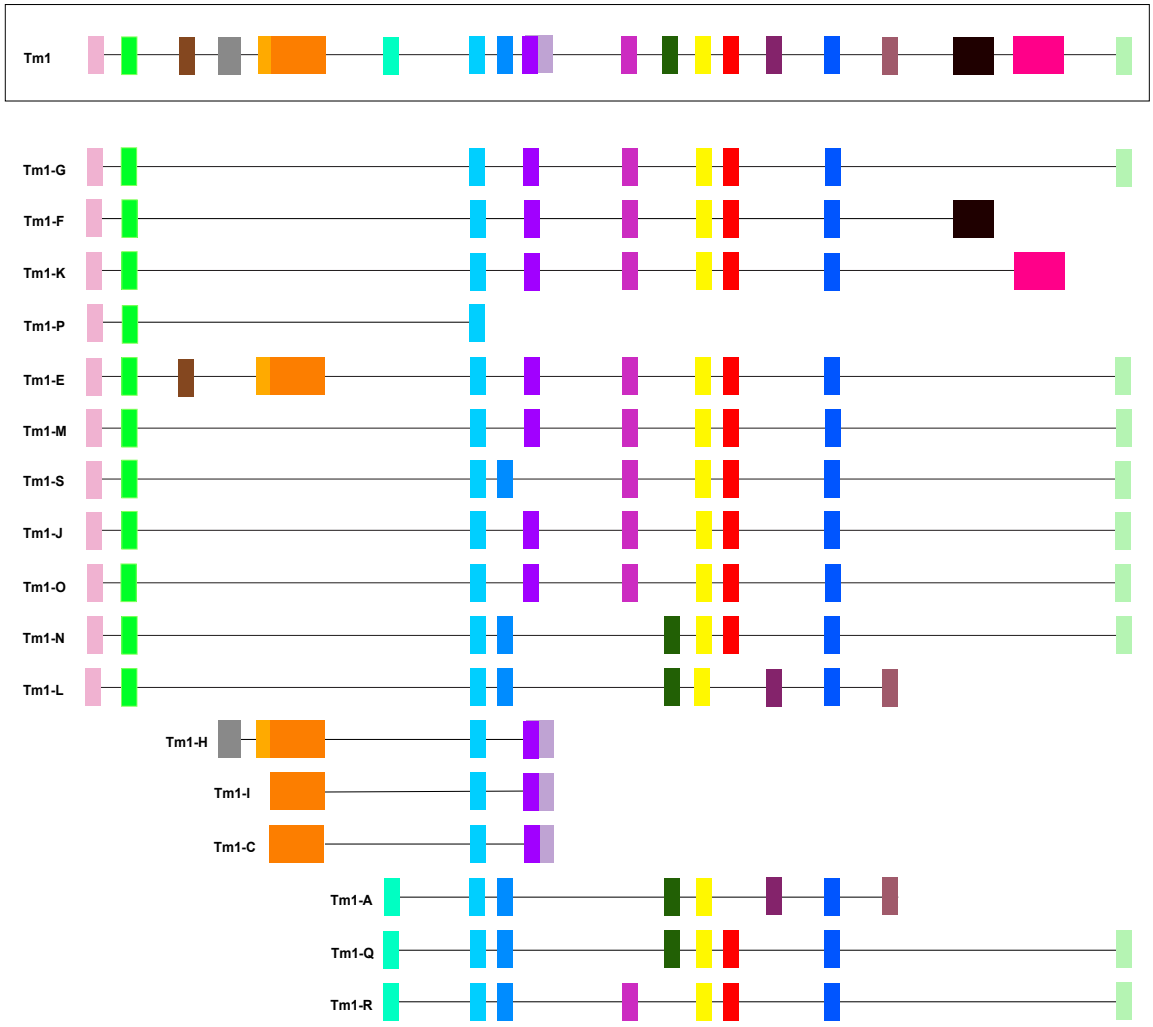
Tm1
Tm1-G
Tm1-F
Tm1-K
Tm1-P
Tm1-E
Tm1-M
Tm1-S
Tm1-J
Tm1-O
Tm1-N
Tm1-L
Tm1-H
Tm1-I
Tm1-C
Tm1-A
Tm1-Q
Tm1-R

Figure 2. Representative coiled coil structure of Tm1 isoforms expressed in *Drosophila* egg chamber

x-axis shows amino acid position and y-axis shows the probability that the sequence will adopt a coiled-coil conformation. Tm1-A (**A**) and Tm1-L (**B**) show end-to-end coil structure whereas Tm1-I (**C**) show partial coiled coil stretch located in the amino acids 270 to 370. The N terminal and C terminal of Tm1-I is composed of random proteins that does not give rise to coiled coil structure.

The structure was determined using COILS program (http://embnet.vital-it.ch/software/COILS_form.html), with MTIDK matrix and window width of 28

A

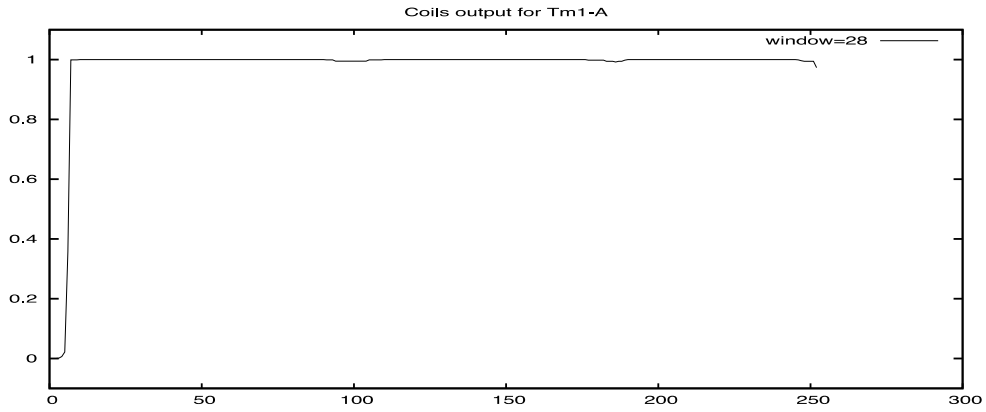
Coils output for Tm1-A
window=28
1
0.8
0.6
0.4
0.2
0
0
50
100
150
200
250
300

B

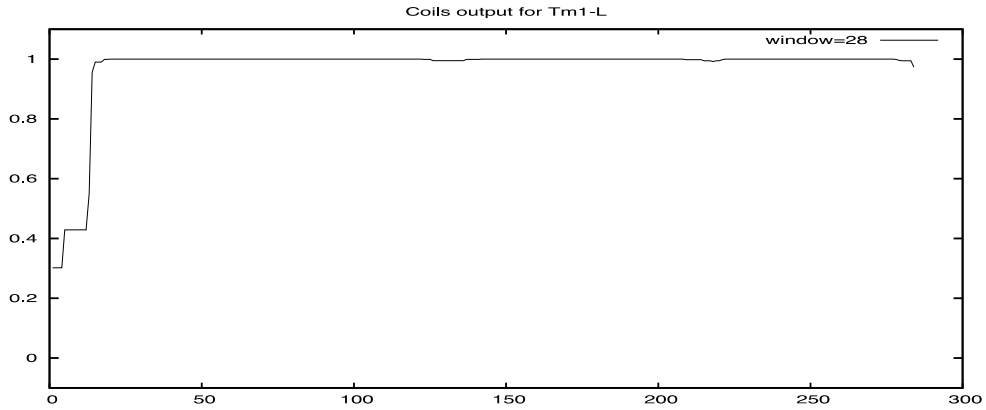
Coils output for Tm1-L
window=28
1
0.8
0.6
0.4
0.2
0
0
50
100
150
200
250
300

C

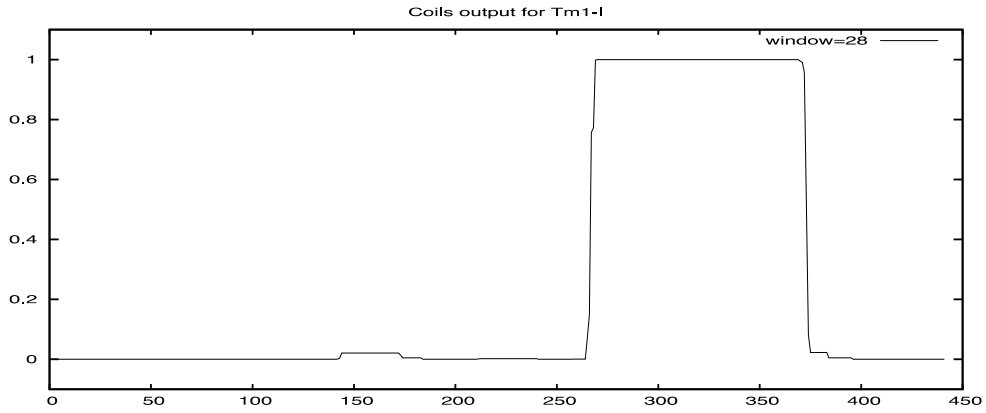
Coils output for Tm1-I
window=28
1
0.8
0.6
0.4
0.2
0
0
50
100
150
200
250
300
350
400
450

Figure 3. RT-PCR result of mRNA tagging experiment

Follicle cell specific mRNA were isolated using slboGal4 driver. Only isoforms Tm1-A, Tm-I and Tm1-L were detected in follicle cells whereas Tm1-C, Tm1-A, Tm1-I, Tm1-Q, Tm1-L, Tm1-P and other muscle forms (Tm1-J, Tm1-N, Tm1-O, Tm1-M, Tm1-S) were detected in mRNAs extracted from whole ovary (positive control). Tm1-H, Tm1-F and Tm1-K were not detected either in control or follicle cells.

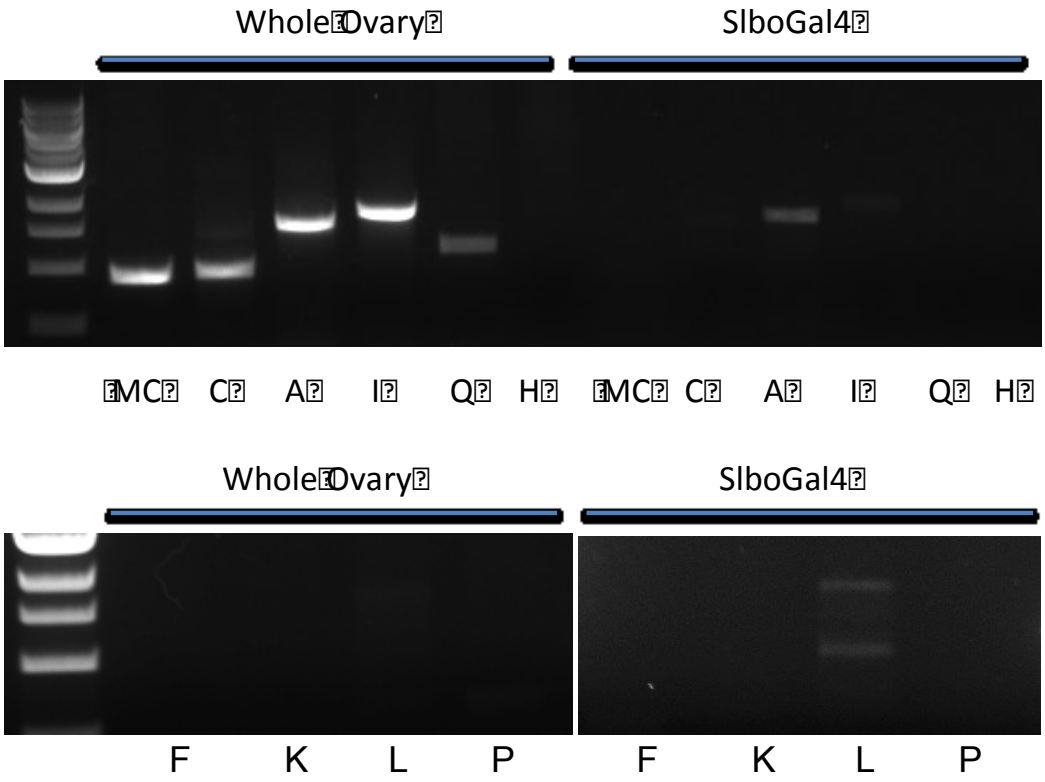

Figure 4. Analysis of commercial Tm monoclonal antibody

Commercial antibody from Abcam was used to detect tropomyosin expression in the egg chambers. The antibody detected protein expressed in the border cells (**A**) and the stress fibers of the epithelial follicle cells (**B**).

(**C**) Western blot analysis. Egg chamber lysate, along with purified His-Tm1-A and His-Tm1-B protein were loaded onto SDS-PAGE gel. The monoclonal antibody detected ~35kDa protein in the egg chamber lysate but did not detect the purified proteins. The same membrane was used to detect His-tagged Tm1-A and Tm1-I using His antibody.

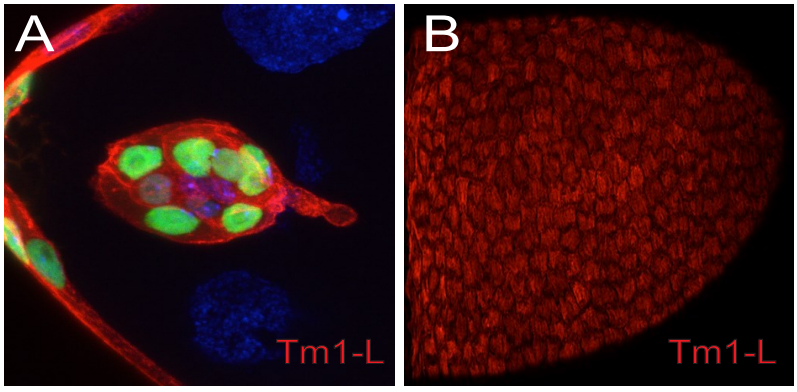
A
Tm1-L
B
Tm1-L

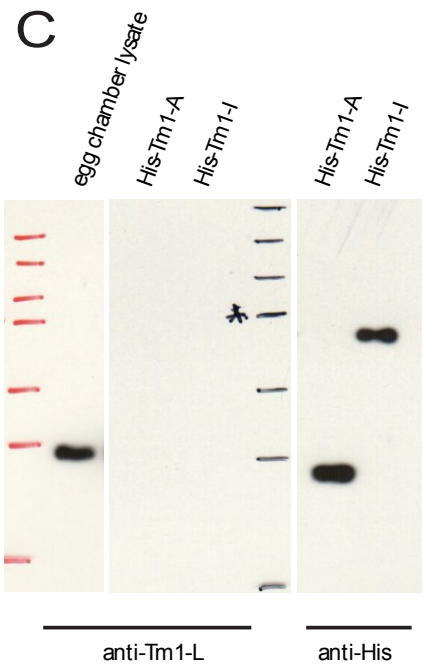
C
egg chamber lysate
His-Tm1-A
His-Tm1-I
His-Tm1-A
His-Tm1-I
anti-Tm1-L
anti-His

Figure 5. Detection of Tm1-L expression using commercial Tm monoclonal antibody

(**A-C**) S2R+ expression of isoforms and detection with HA and Tm1-L antibody. HA-PA (**A**), HA-PI (**B**), and HA-PL (**C**) were detected using anti-HA antibody. Among the transfected constructs, only HA-PL was detected by Tm1-L antibody (**C''**).

(**D**) Overexpression of HA-PL in egg chambers. The HA-PL construct was overexpressed in subset of follicle cells. Tm1-L antibody detected the overexpressed construct (**D'**) which colocalized with HA antibody staining (**D''**)

(**E**) Expression of muscle Tm isoforms in muscle sheath enclosing the egg chamber. Phalloidin stains the actin filaments (red) and muscle Tm wraps around the actin filament (green).

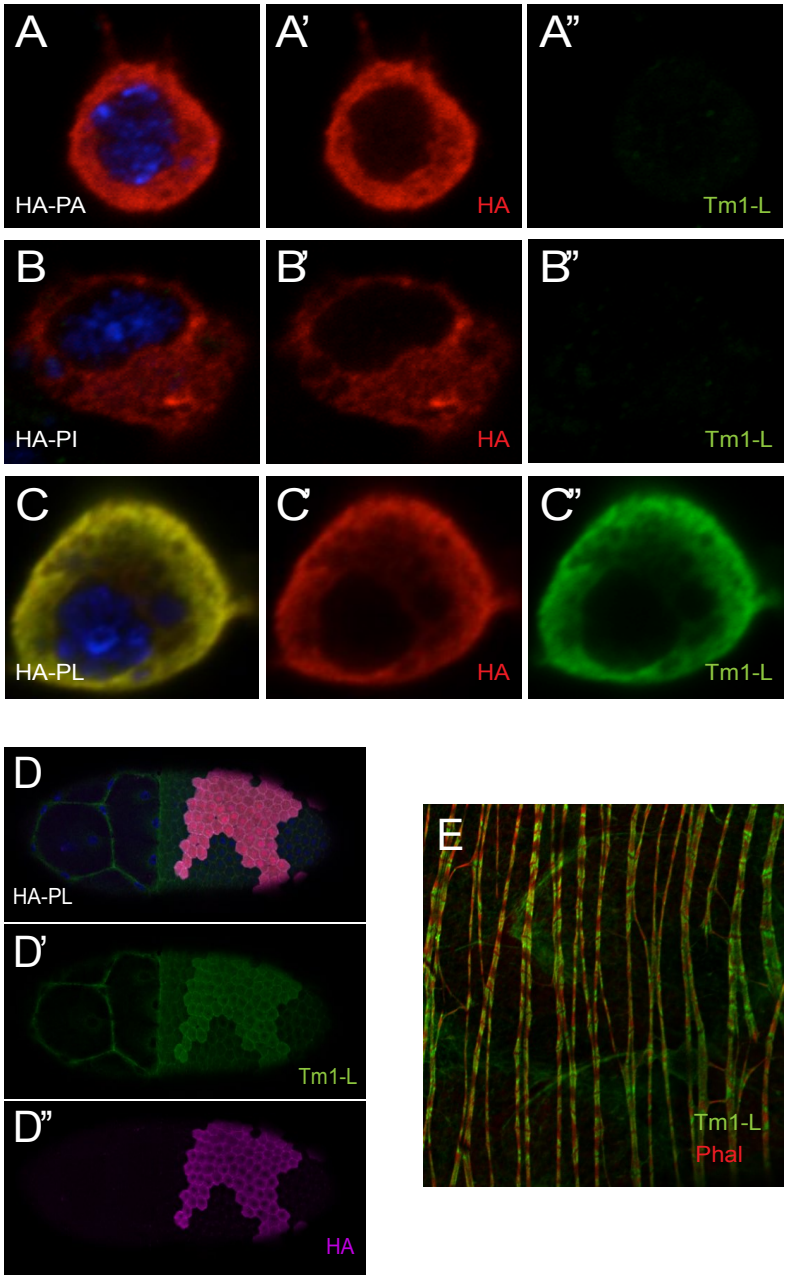
A
HA-PA
A'
HA
A"
Tm1-L
B
HA-PI
B'
HA
B"
Tm1-L
C
HA-PL
C'
HA
C"
Tm1-L
D
HA-PL
D'
Tm1-L
D"
HA
E
Tm1-L
Phal

Figure 6. Tm1-A and Tm1-I are expressed in the egg chamber

(**A**) Tm1-A expression in egg chamber. Tm1-A is highly expressed in follicle cells including border cells. Since protein composition of Tm1-A and Tm1-L highly overlap, Tm1-A also detects Tm1-L.

(**B**) Tm1-I expression in egg chamber. Tm1-I is highly expressed in follicle cells and germline cells. Tm1-I shows strong expression in nurse cells, in the cytoplasm and in the nurse cell – nurse cell junctions. Localization of Tm1-I is also detected in the posterior of the oocyte (arrow).

Scale bar, 50μm

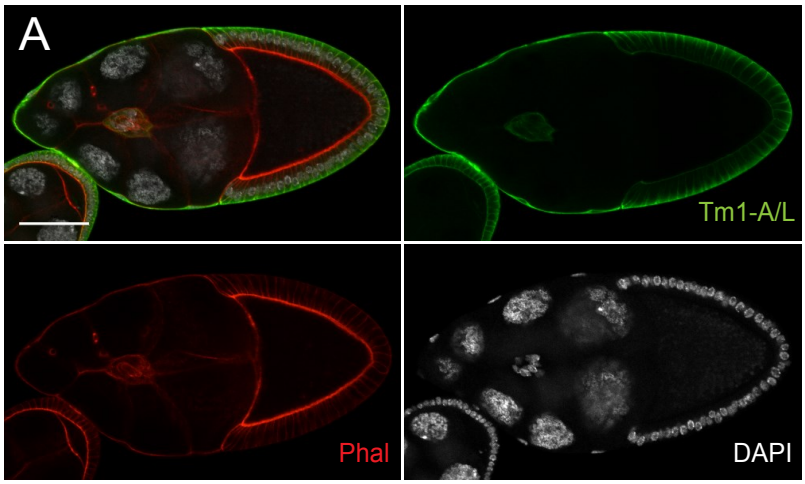
A
Tm1-A/L
Phal
DAPI

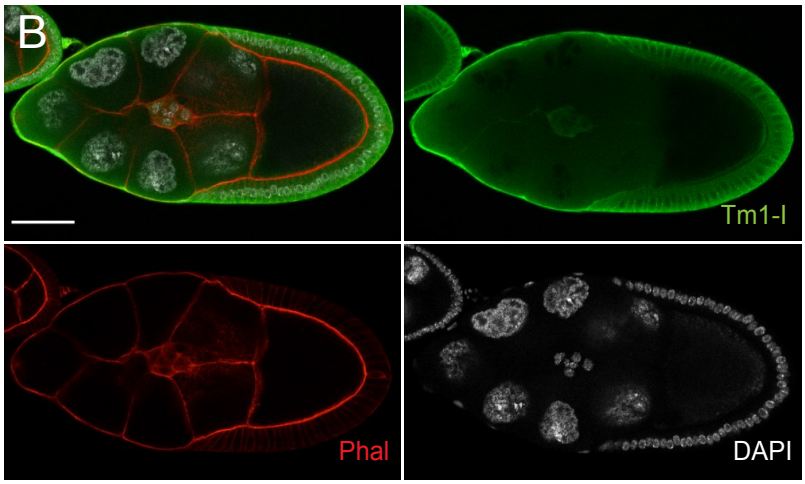
B
Tm1-I
Phal
DAPI

Figure 7. Specificity of Tm1-A/L and Tm1-I antibodies

(**A**) Western analysis of purified His-Tm1-A and His-Tm1-I. Two purified proteins were blotted with Anti-Tm1-A and Anti-Tm1-I. Anti-Tm1-A only detected purified Tm1-A but not Tm1-I. Anti-Tm-I only detected purified Tm1-I but not Tm1-A, showing that the antibodies are specific for each antibody.

(**B**) EGFP-Tm1-A is overexpressed in subset of follicle cells. Tm1-A/L antibody recognizes the overexpressed Tm-A (**B**').

(**C**) EGFP-Tm1-I is overexpressed in subset of follicle cells. Tm1-I antibody detects the Tm1-I in the follicle cells and also the overexpressed Tm-I (**C'**)

Scale bar, 10 μm

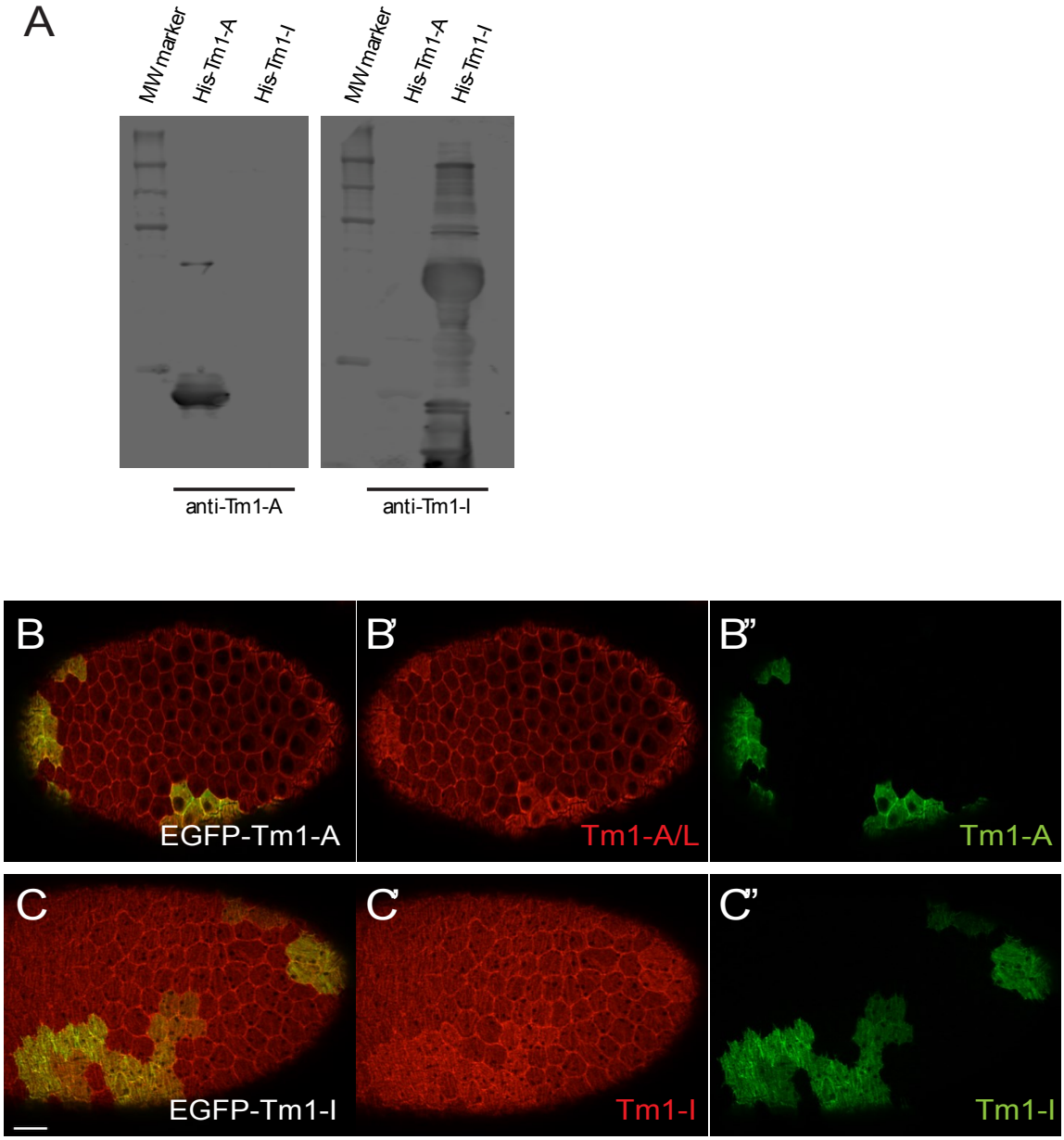
A
MW marker
His-Tm1-A
His-Tm1-I
MW marker
His-Tm1-A
His-Tm1-I
anti-Tm1-A
anti-Tm1-I
B
EGFP-Tm1-A
B'
Tm1-A/L
B"
Tm1-A
C
EGFP-Tm1-I
C'
Tm1-I
C"
Tm1-I

Figure 8. Tm1 isoforms are highly expressed on the stress fibers in the basal layer of the epithelial follicle cells

Wild type egg chambers were used and different Tm1 isoforms were detected using isoform specific antibodies. Phalloidin (red) is used to detect the actin structures in the follicle cells.

(**A**) Tm1-L is expressed on the stress fibers. The image is from stage 11 egg chamber. In this stage, Tm1-L is highly expressed on the membrane of the follicle cell.

(**B**) Tm1-I is expressed on the stress fibers. During stage 10, the Tm1-I is excluded from the cortical actin structures and only expressed on the stress fibers.

(**C**) Tm1-A localizes to the stress fibers and the cortical actin structures. Since Tm1-A/L antibody recognizes both Tm1-A and Tm1-L, (C'') shows both isoforms.

Scale bar, 10 μm

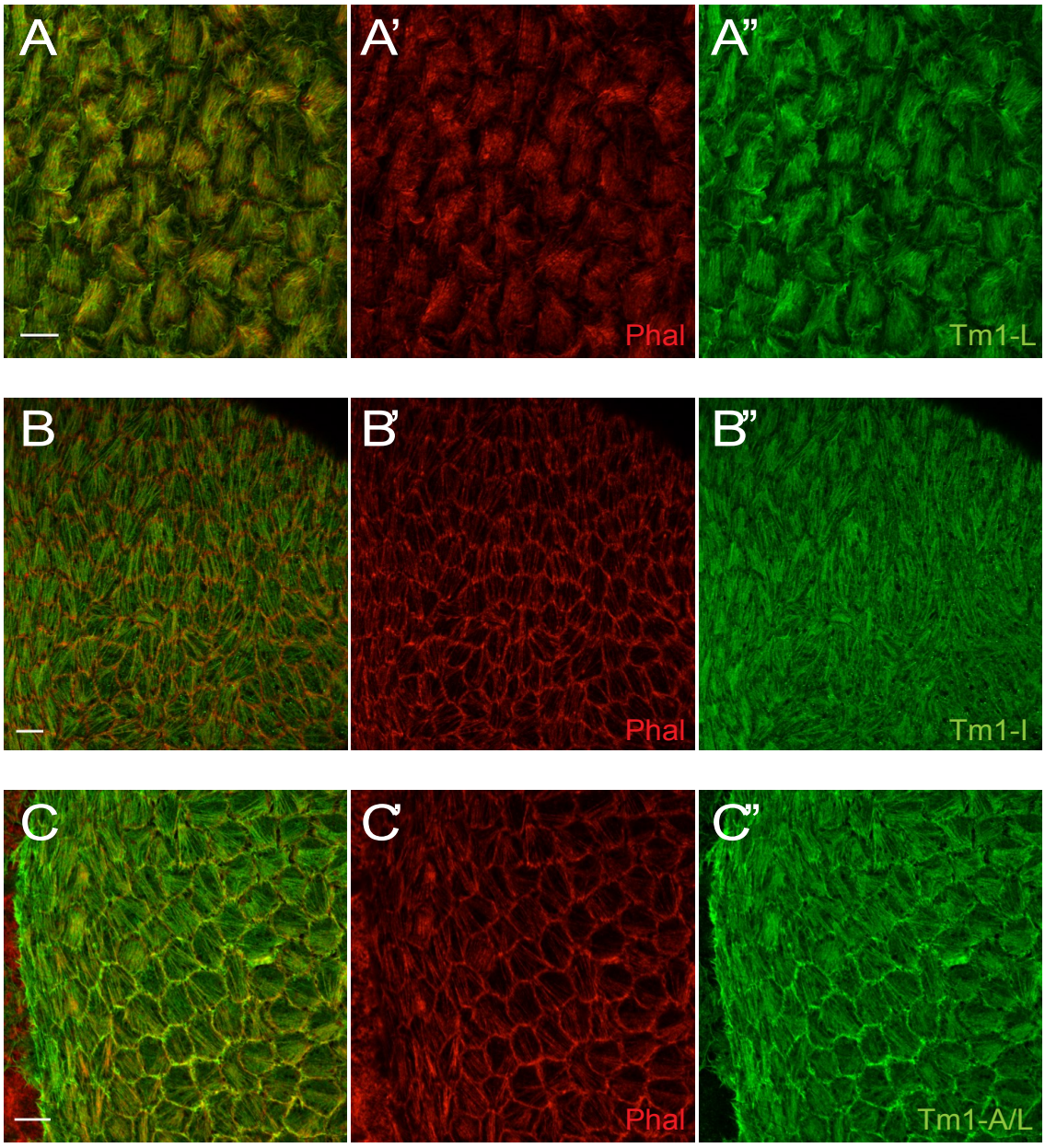
A
A'
A"
Phal
Tm1-L
B
B'
B"
Phal
Tm1-I
C
C'
C"
Phal
Tm1-A/L

Figure 9. Tm1 mutant border cells show migration defect

(**A-D**) Stage 10 control and Tm1 mutant egg chambers. Homozygous mutant follicle cells (GFP+) are generated by MARCM. DAPI (blue) stains the nucleus and phalloidin (red) detects the actin filaments. Compared to control, where border cells reached the border of the oocyte by stage 10 (**A**), different homozygous mutant Tm1 border cells show incomplete migration (**B-D**).

(**E**) Quantification of border cell migration defect. Percentage of stage 10 egg chambers with border cells migration defect was counted. Red bar indicates no migration, yellow bar migrated less than 50%, blue bar migrated more than 50% but not complete and green bar indicates complete migration. 95% of control egg chambers had border cells complete their migration. About 50~80% of egg chambers with different homozygous mutant Tm1 border cells showed incomplete migration.


A
control
B
Tm1su(flw)4
C
Tm1zcl0722
D
Tm1pz2299

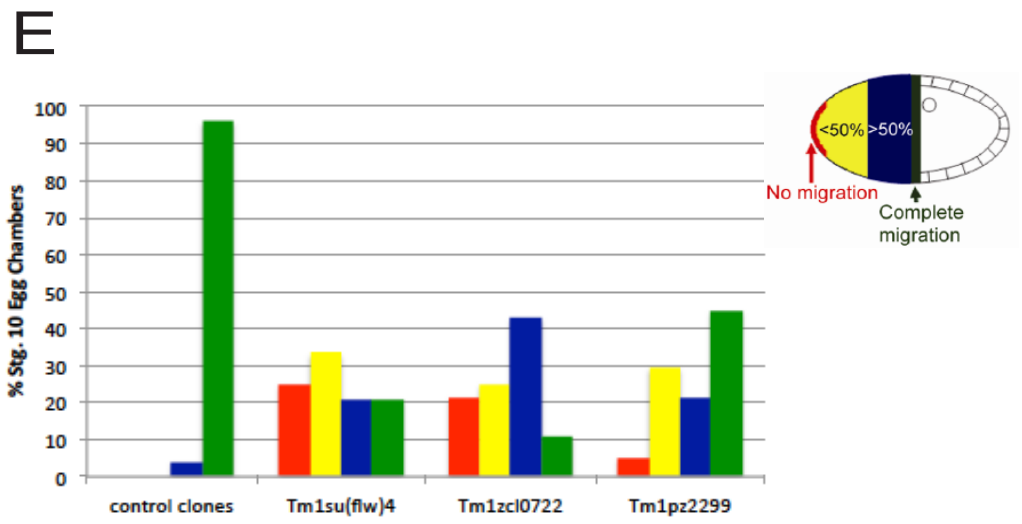
E
% Stg. 10 Egg Chambers
100
90
80
70
60
50
40
30
20
10
0
control clones
Tm1su(flw)4
Tm1zcl0722
Tm1pz2299
<50%
>50%
No migration
Complete migration

Figure 10. Tm1 null follicle cells show absence of Tm1-L, Tm1-A and Tm-I expression

(**A**) Tm1 null line is made by homologous recombination. Tm1 gene and its exon composition are shown. The exon that is common to all isoform (sky blue) is replaced with w+ gene.

(**B**) Tm1-L expression detected with Tm1-L antibody. Homozygous Tm1 null cells (GFP positive) show absence of Tm1-L expression compared to GFP negative wild type cells.

(**C**) Tm1-A/L expression is detected with Tm1-A/L antibody. Homozygous Tm1 null cells (GFP positive) show absence of Tm1-A/L expression compared to GFP negative wild type cells.

(**D**) Tm1-I expression detected with Tm1-I antibody. Homozygous Tm1 null cells (GFP positive) show highly reduced Tm1-I expression compared to GFP negative wild type cells.

Scale bar, 10 μm

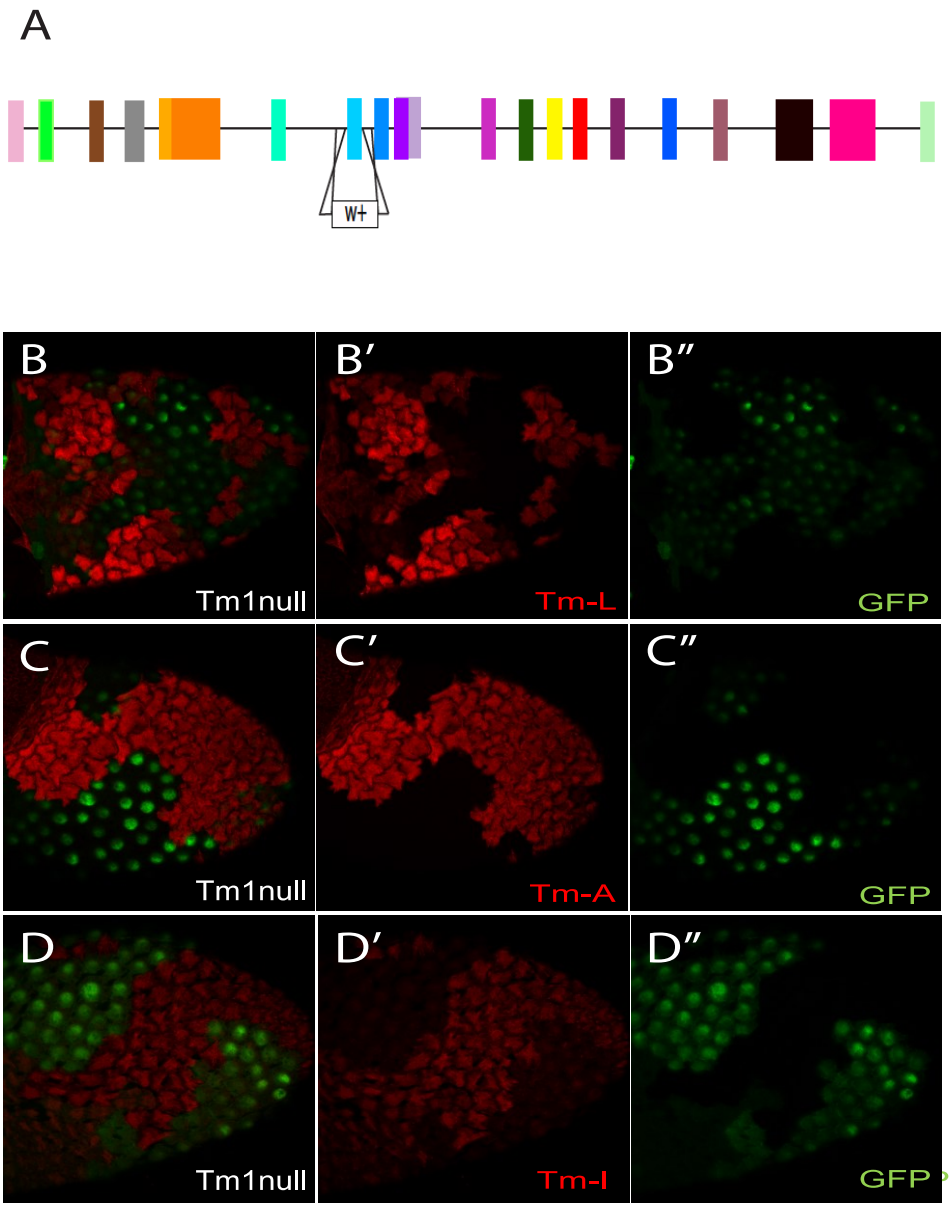
A
W+
B
Tm1null
B′
Tm-L
B″
GFP
C
Tm1null
C′
Tm-A
C″
GFP
D
Tm1null
D′
Tm-I
D″
GFP

Figure 11. Tm1 null border cells show absence of Tm1-L, Tm1-A and Tm-I expression.

Border cell cluster with subset of cells that is homozygous mutant border cell were generated using MARCM protocol with Tm1 null flies. In all samples, GFP positive cells are homozygous null cells; nucleus is marked with DAPI and Tm1 isoform staining is shown in red.

(**A**) Tm1-L expression (**B**) Tm1-A\L expression (**C**) Tm1-I expression.

(**D**) Quantification of Tm1 null border cell migration defect. Only whole homozygous null border cells were counted for migration defect. 70% of the stage 10 egg chambers with homozygous null border cells showed border cell migration defect.

Scale bar, 10 μm

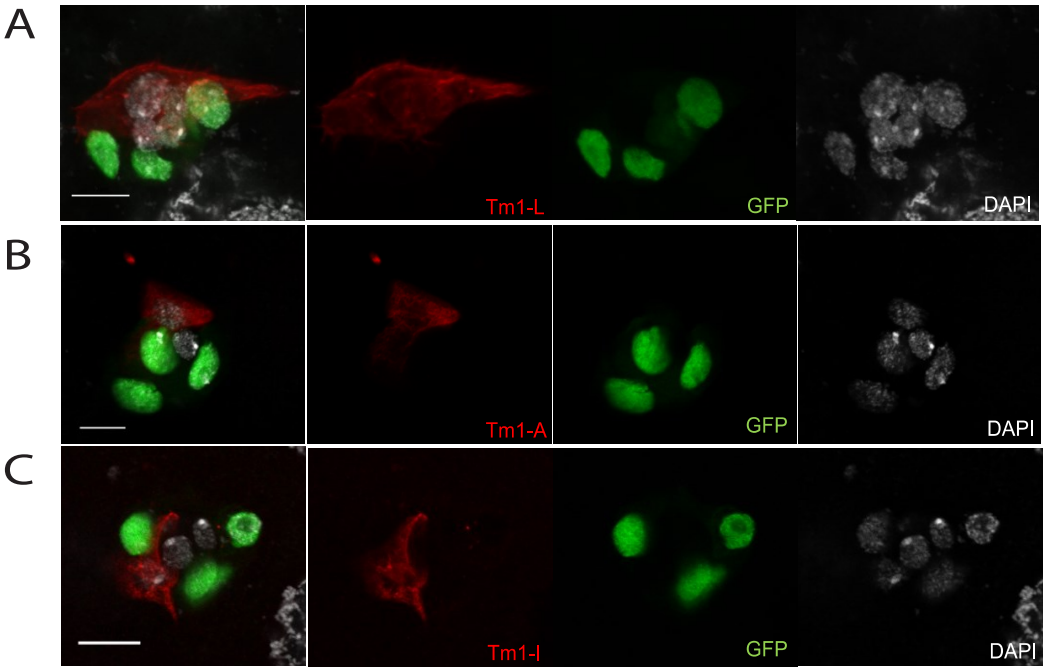
A
Tm1-L
GFP
DAPI
B
Tm1-A
GFP
DAPI
C
Tm1-I
GFP
DAPI

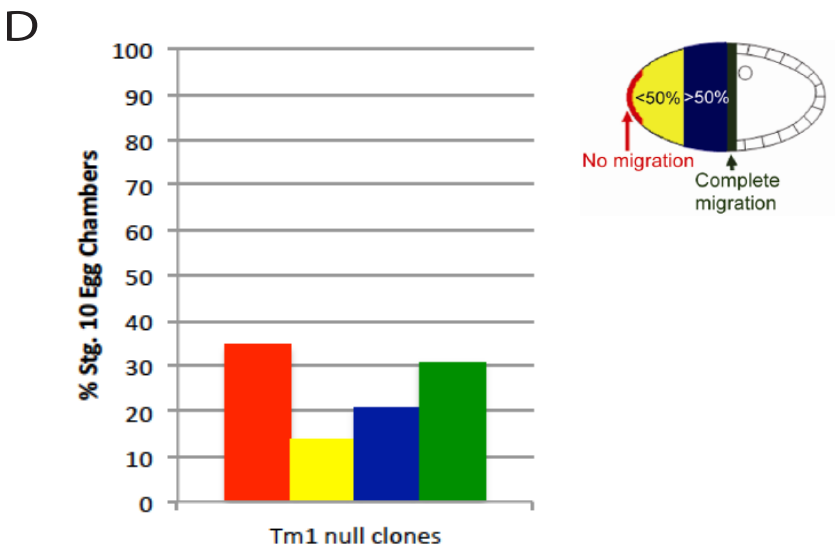
D
100
90
80
70
60
50
40
30
20
10
0
% Stg. 10 Egg Chambers
Tm1 null clones
<50%
>50%
No migration
Complete migration

Figure 12. Tm1-A functions in border cell migration

(**A**) Quantification of $Tm1^{pz2299}$ and Tm1-A RNAi migration defect. 60% of stage 10 egg chambers that has homozygous $Tm1^{pz2299}$ mutant border cells showed migration defect. Re-expressing Tm1-A restored the migration completion to 70% whereas re-expressing Tm1-I did not have significant effect. Tm1-A RNAi expressing border cells showed normal migration activity.

(**B**) Reduction of Tm1-A determined by Tm1-A/L antibody (**B'**) in $Tm1^{pz2299}$ homozygous mutant follicle cells (**B''**).

(**C**) Reduction of Tm1-A determined by Tm1-A/L antibody (**C'**) in Tm1-A RNAi expressing follicle cells (**C''**)

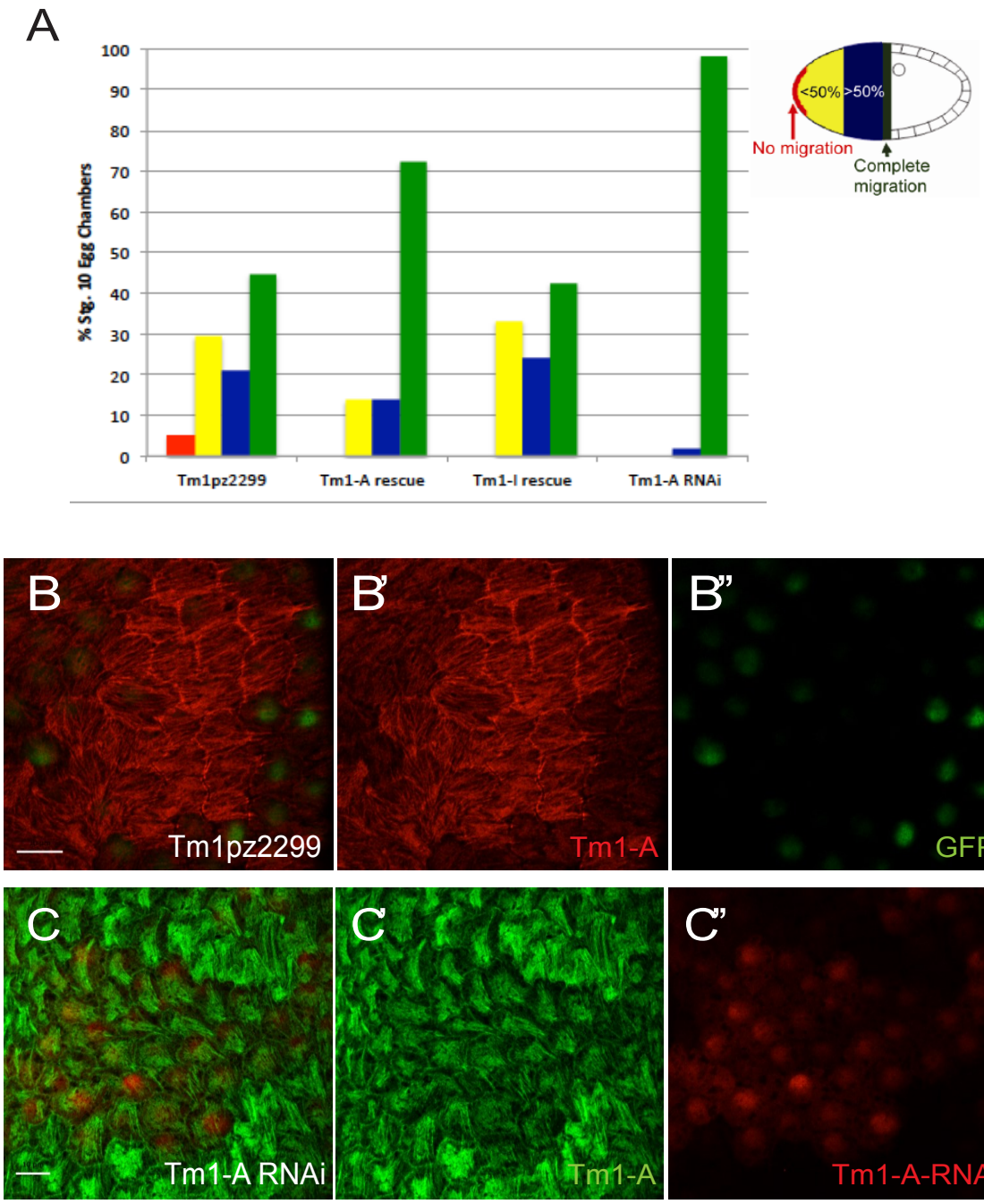
A
100
90
80
70
60
50
40
30
20
10
0
% Stg. 10 Egg Chambers
Tm1pz2299
Tm1-A rescue
Tm1-I rescue
Tm1-A RNAi
<50%
>50%
No migration
Complete migration
B
Tm1pz2299
B'
Tm1-A
B"
GFP
C
Tm1-A RNAi
C'
Tm1-A
C"
Tm1-A-RNAi

Figure 13. Tm1 isoform expressions in $Tm1^{su(flw)4}$ homozygous mutant follicle cells

(**A**) Level of Tm1-I detected with Tm1-I antibody in homozygous $Tm1^{su(flw)4}$ mutant cells. GFP positive cells are homozygous mutant cells. Compared to wild type cells (GFP negative), homozygous mutant cells show reduction of Tm1-I (**A'**).

(**B**) Level of Tm1-A/L in $Tm1^{su(flw)4}$ mutant cells detected with Tm1-A/L antibody. GFP positive cells are homozygous $Tm1^{su(flw)4}$ mutant. The mutant cells show slight increase in Tm1-A/L level in the apical layer of the follicle cells compared to neighboring wild type cells (GFP negative). Also, smaller follicle cells are noticeable in homozygous $Tm1^{su(flw)4}$ mutant cells.

(**C**) Level of Tm1-L in $Tm1^{su(flw)4}$ mutant cells detected with Tm1-L antibody. GFP positive cells (**C''**) are homozygous $Tm1^{su(flw)4}$ mutant. The mutant cells show slight increase in Tm1-L level in the apical layer of the follicle cells compared to neighboring wild type cells (GFP negative).

Scale bar, 10 μm

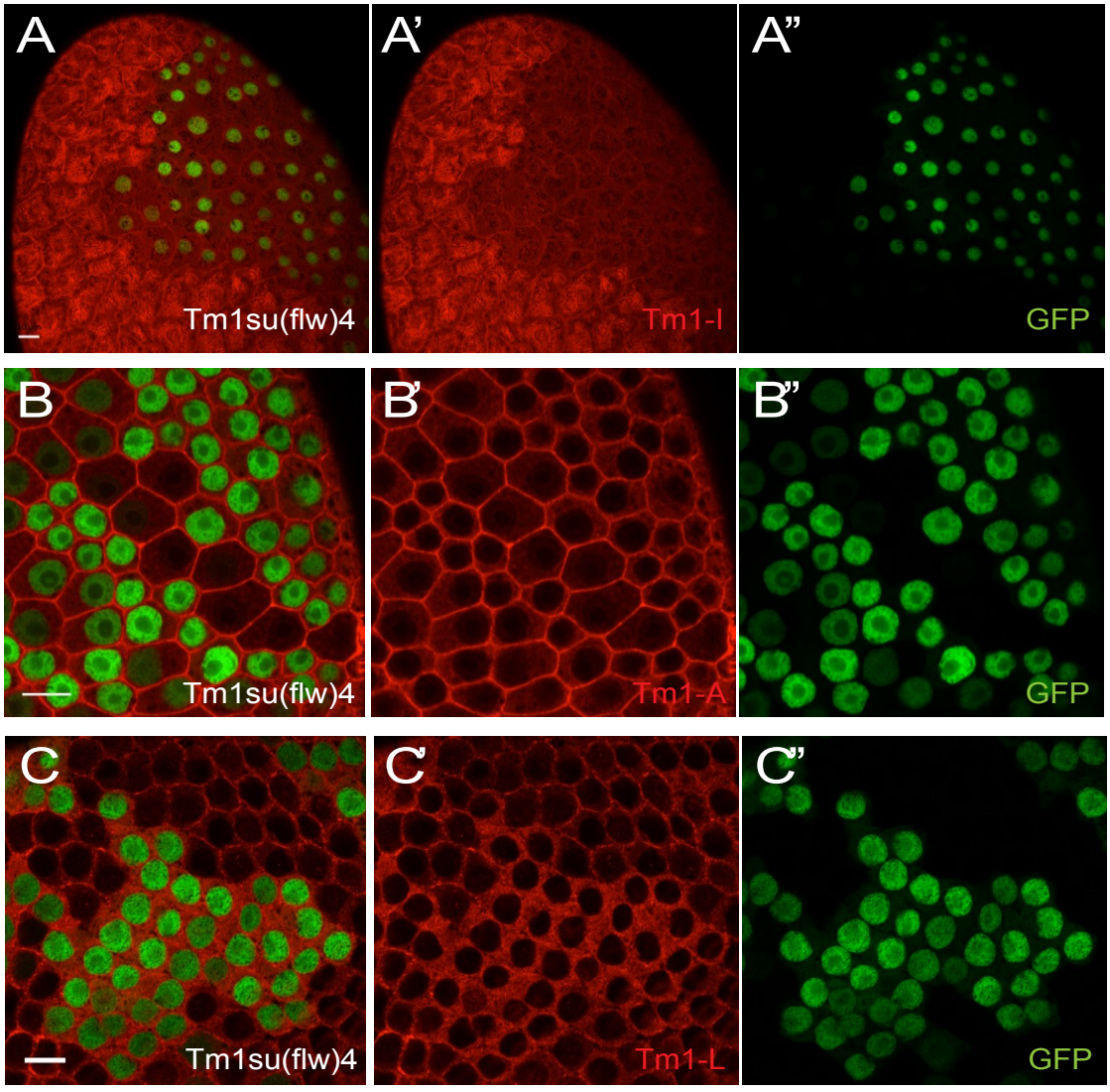
A
Tm1su(flw)4
A'
Tm1-I
A"
GFP
B
Tm1su(flw)4
B'
Tm1-A
B"
GFP
C
Tm1su(flw)4
C'
Tm1-L
C"
GFP

Figure 14. Tm1-I functions in border cell migration

(**A**) Quantification of $Tm1^{su(flw)4}$ and Tm1-A RNAi migration defect. 80% of stage 10 egg chambers that has homozygous $Tm1^{su(flw)4}$ mutant border cells showed migration defect. Re-expressing Tm1-A did not effect border cell migration such that migration defect was comparable to $Tm1^{su(flw)4}$ clones. However, re-expressing Tm1-I rescued the border cell migration defect, resulting in 80% of stage 10 egg chambers completing migration. 40% of stage 10 egg chambers that expressed Tm1-I RNAi also showed border cell migration defect.

(**B**) Level of Tm1-I is reduced in Tm1-I RNAi expressing follicle cells, showing that Tm1-I RNAi targets the I isoform to knock down the level of the protein.

A

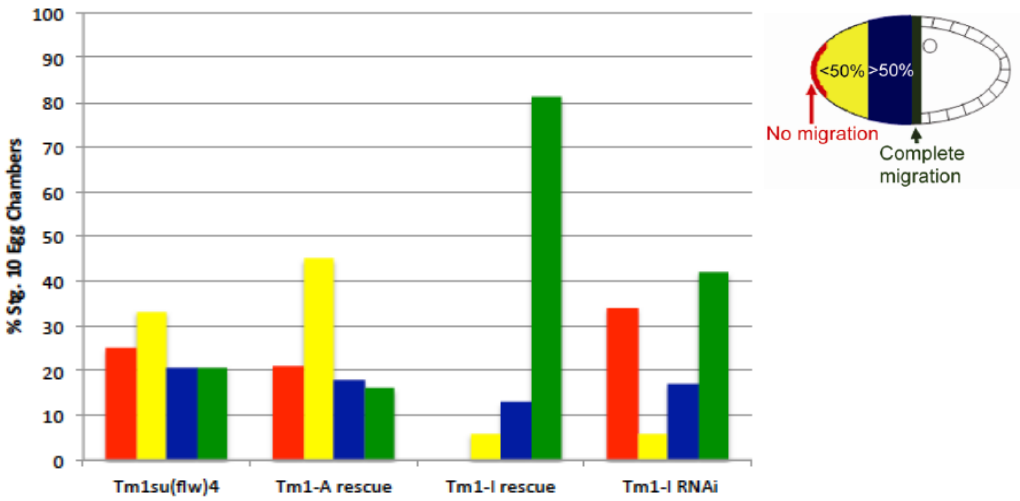
100
90
80
70
60
50
40
30
20
10
0
% Stg. 10 Egg Chambers
Tm1su(flw)4
Tm1-A rescue
Tm1-I rescue
Tm1-I RNAi
<50%
>50%
No migration
Complete migration

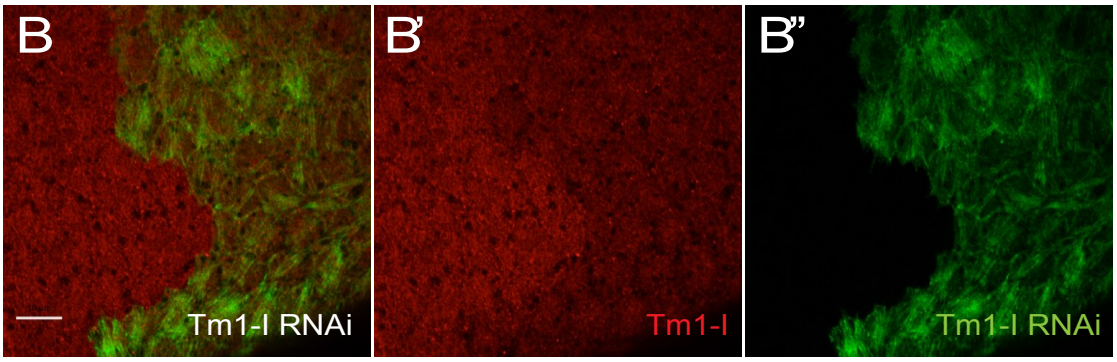
B
Tm1-I RNAi
B'
Tm1-I
B"
Tm1-I RNAi

Figure 15. Tm1-L is not required for border cell migration

(**A**) Border cell cluster with subset of cells expressing Tm1-L RNAi. Tm1-L expression (**A'**) is absent only in cells where Tm1-L RNAi is expressed (A'', GFP positive cells) Scale bar, 10 μm

(**B**) Quantification of border cell migration index in Tm1-L knock down cells. Control (slbo-Gal4, LifeAct-GFP) and Tm1-L RNAi expressed with slbo-Gal4, LifeAct-GFP show comparable border cell migration completion (~93%) in stage 10 egg chambers.

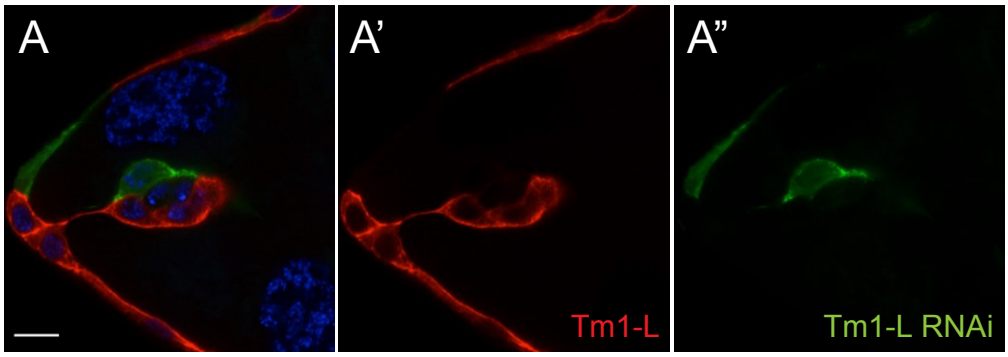
A
A'
A"
Tm1-L
Tm1-L RNAi

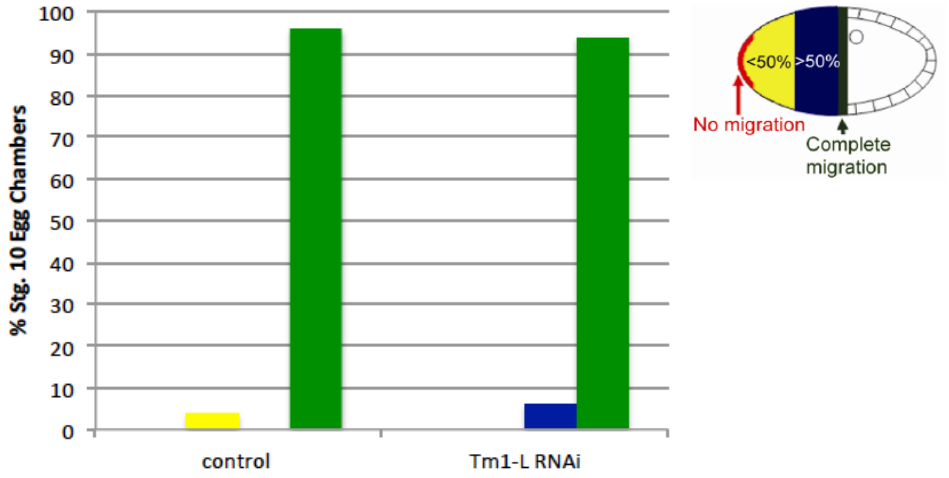
% Stg. 10 Egg Chambers
100
90
80
70
60
50
40
30
20
10
0
control
Tm1-L RNAi
<50%
>50%
No migration
Complete migration

Figure 16. Tml null clones show reduced stress fibers but increased Myosin II accumulation

(**A**) Level of actin filaments detected by phalloidin staining in Tm1 null homozygous mutant cells. . GFP positive cells are homozygous mutant cells for Tm1. Compared to GFP negative wild type cells, GFP positive cells show decrease in phalloidin (RFP) staining indicating reduction of actin filaments in mutant cells.

(**B**) Level of non-muscle myosin light chain detected by sqh-mcherry in Tm1 null homozygous mutant cells. GFP positive cells are homozygous mutant cells for Tm1. Compared to wild type cells (GFP negative), GFP positive cells show increase in mcherry staining, indicating high level of non-muscle myosin activity.

(**C**) Quantification of sqh-mcherry and phalloidin (RFP) level in mutant and wild type cells. Sqh-mcherry level shows almost 2-fold increase while phalloidin level is reduced about 40%.

Scale bar, 10 μm

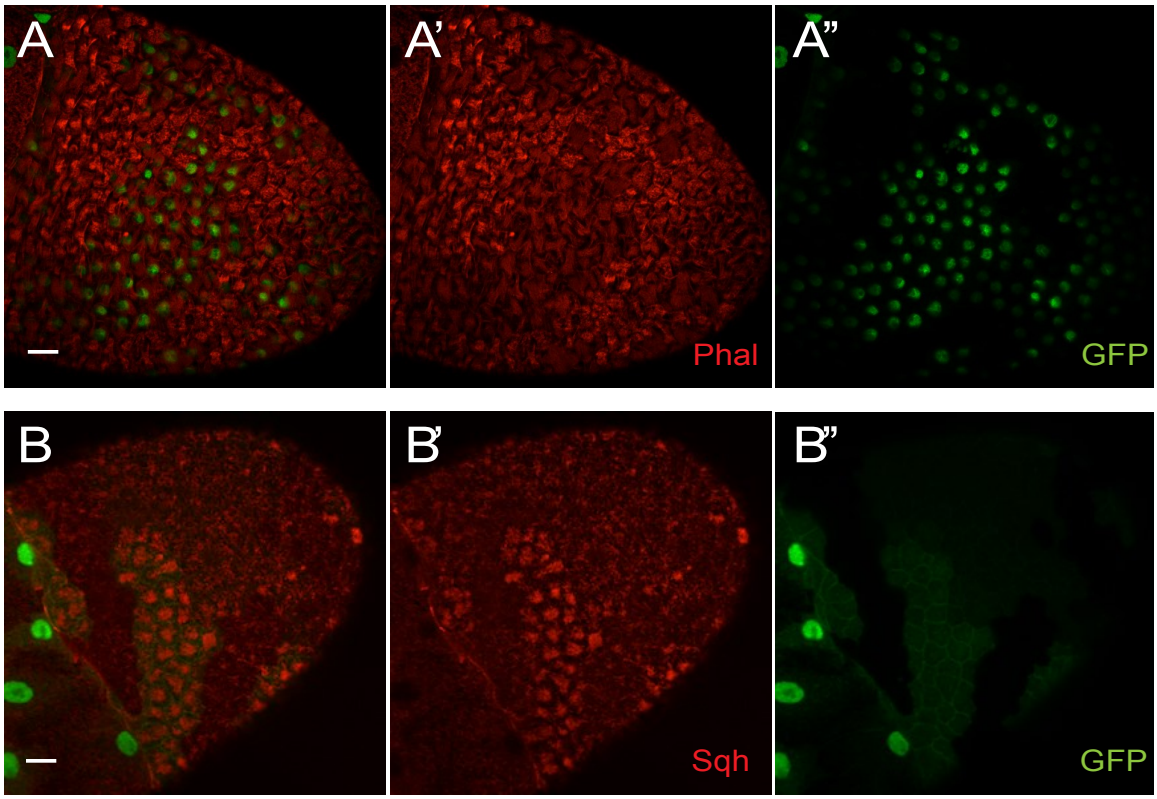
A
A'
A"
Phal
GFP
B
B'
B"
Sqh
GFP

C

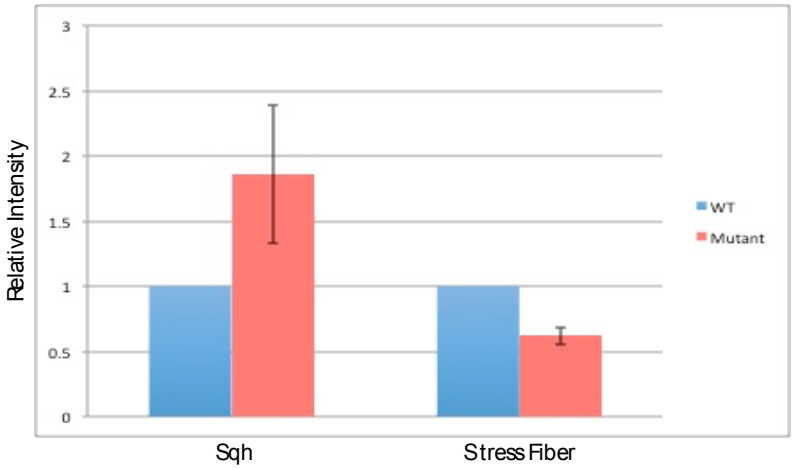
Relative Intensity
3
2.5
2
1.5
1
0.5
0
WT
Mutant
Sqh
Stress Fiber

Figure 17. Tm1-A or Tm1-L is not required for stress fiber regulation

(**A**) Level of actin filament detected by phalloidin staining in homozygous $Tm1^{pz2299}$ mutant cells. GFP positive cells are homozygous mutant cells. These cells show comparable level of actin filaments with wild type cells (GFP negative).

(**B**) Level of actin filament detected with phalloidin staining in Tm1-A RNAi expressing cells. Tm1-A RNAi is expressed in RFP positive cells. Tm1-A reduced cells and wild type cells show comparable level of actin filaments.

(**C**) Follicle cell clone with Tm1-L RNAi expression. Tm1-L expression (**C'**) is absent only in cells where Tm1-L RNAi is expressed (**C''**, RFP positive cells)

(**D**) Phalloidin staining to show actin filament expression. Phalloidin staining of actin bundles (**D'**) show unaltered in Tm1-L RNAi is expressing RFP positive cells (**D''**)

Scale bar, 10 μm

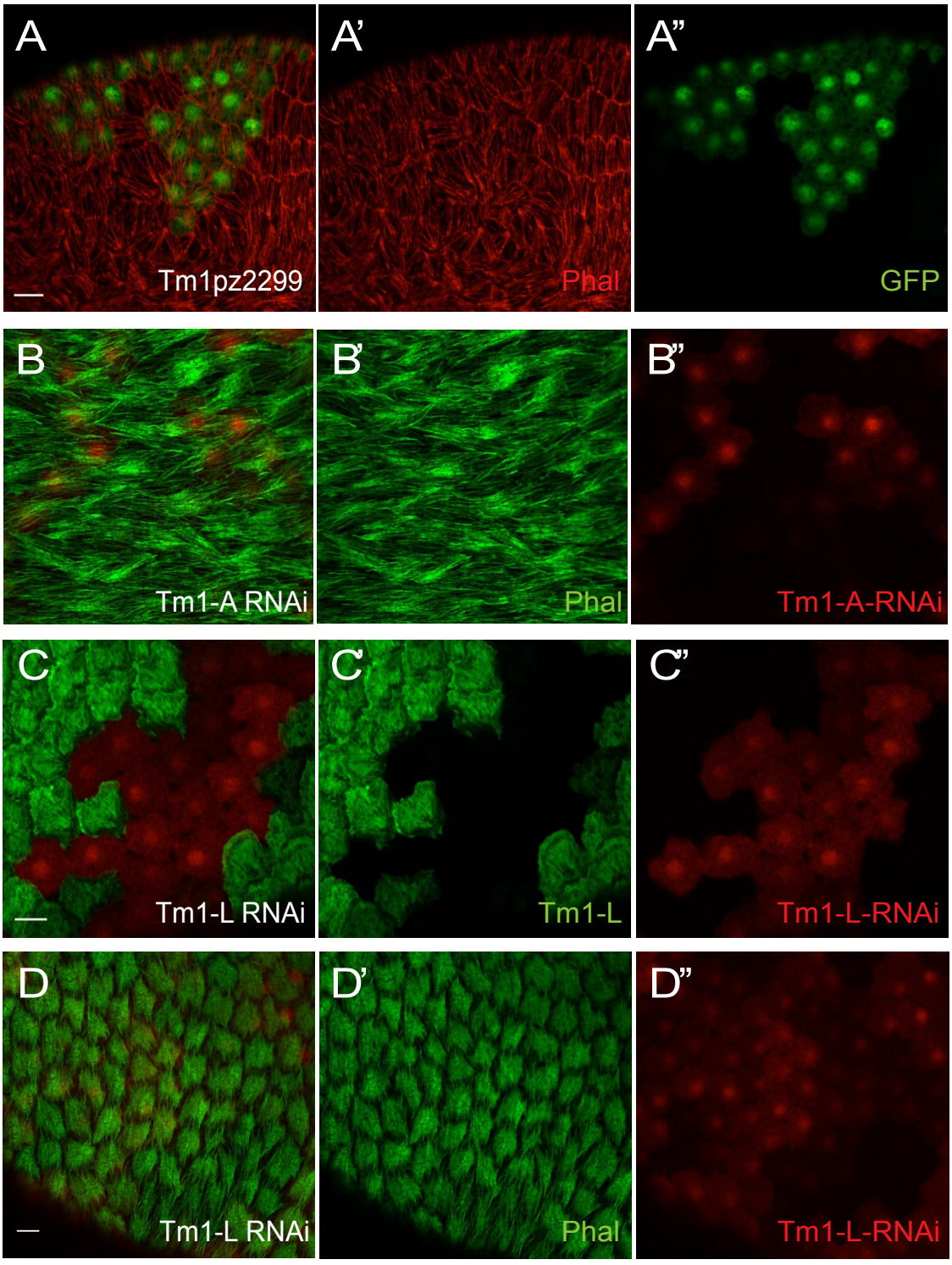
A
Tm1pz2299
A'
Phal
A"
GFP
B
Tm1-A RNAi
B'
Phal
B"
Tm1-A-RNAi
C
Tm1-L RNAi
C'
Tm1-L
C"
Tm1-L-RNAi
D
Tm1-L RNAi
D'
Phal
D"
Tm1-L-RNAi

Figure 18. Tm1-I regulates stress fibers and Myosin II accumulation

(A) Level of actin filament detected by phalloidin staining in Tm1-I RNAi expressing cells GFP positive. Cells with reduced Tm1-I show reduction in actin filaments detected by phalloidin staining **(A')**.

(B) Level of non-muscle myosin light chain detected by phosphorylated non-muscle myosin light chain antibody in Tm1-I RNAi expressing GFP positive cells.. Cells with reduced Tm1-I show 40% reduction in myosin light chain activity **(B')** compared to wild type cells.

(C) Level of actin filament detected by phalloidin staining in homozygous $Tm1^{su(flw)4}$ mutant cells. GFP positive cells are homozygous mutant cells. Compared to wild type cells (GFP negative), homozygous mutant cells show 40% reduction of actin filaments detected with phalloidin staining **(C')**.

(D) Level of non-muscle myosin light chain detected by sqh-mcherry in $Tm1^{su(flw)4}$ homozygous mutant cells. GFP positive cells are homozygous mutant cells. Compared to wild type cells (GFP negative), GFP positive cells show 40% reduction of mcherry staining, indicating reduced level of non-muscle myosin activity **(D')**.

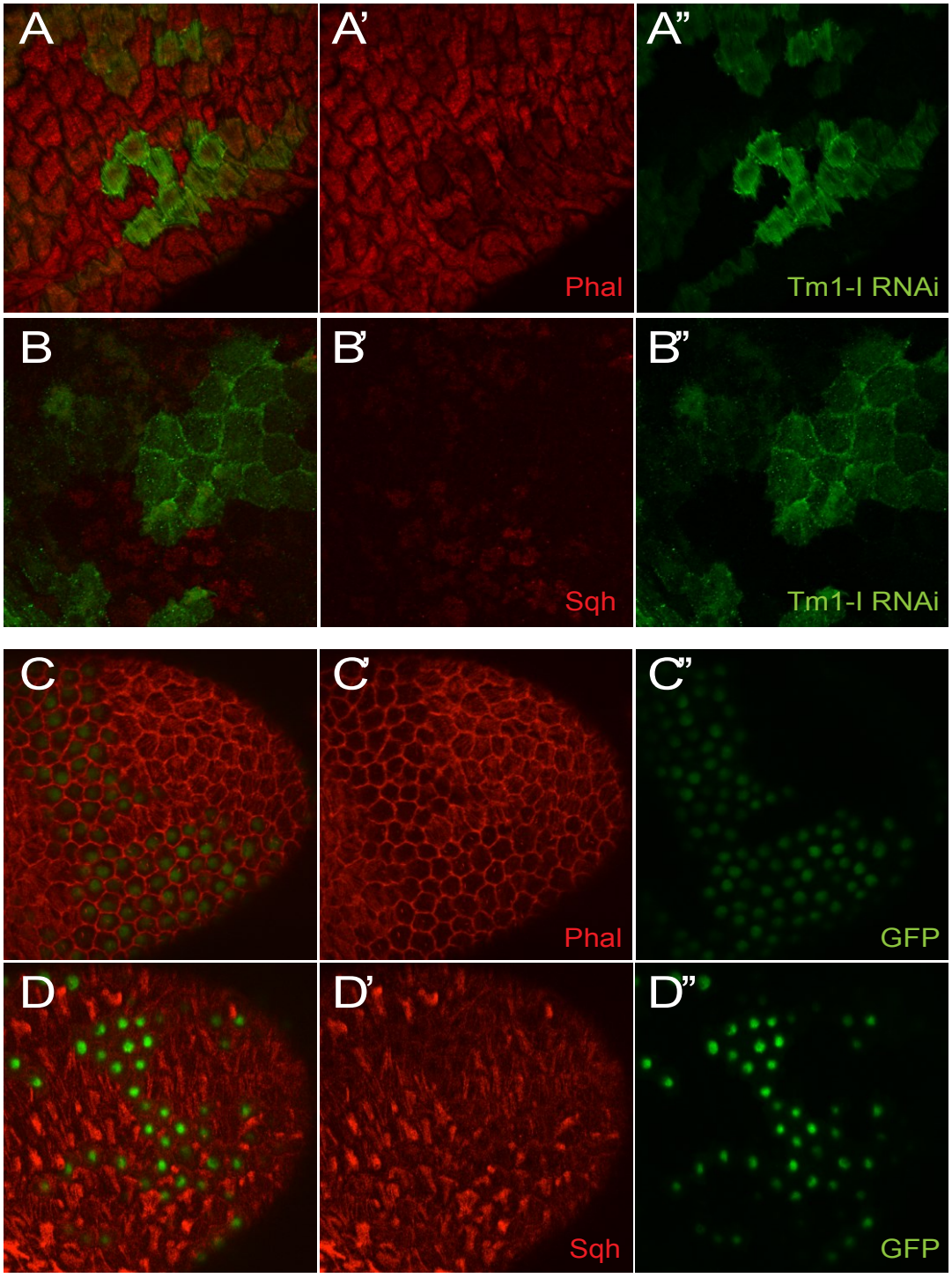
A
A'
A"
Phal
Tm1-I RNAi
B
B'
B"
Sqh
Tm1-I RNAi
C
C'
C"
Phal
GFP
D
D'
D"
Sqh
GFP

Figure 19. $Tm1^{su(flw)4}$ mutant follicle cells show reduced cell area

(A) $Tm1^{su(flw)4}$ homozygous mutant follicle cells are indicated by the absence of GFP expression. Phalloidin staining marks the actin structures **(A')**.

(B) Quantification of cell area. GFP positive wild type cells and GFP negative $Tm1^{su(flw)4}$ homozygous mutant follicle cell area was measured with ImageJ. Since follicle cells vary in their size according their location in the egg chamber, we specifically selected wild type and mutant cells that are side by side and compared their area. Compared to the wild type cells, $Tm1^{su(flw)4}$ homozygous mutant follicle cells showed 40% reduction in cell area.

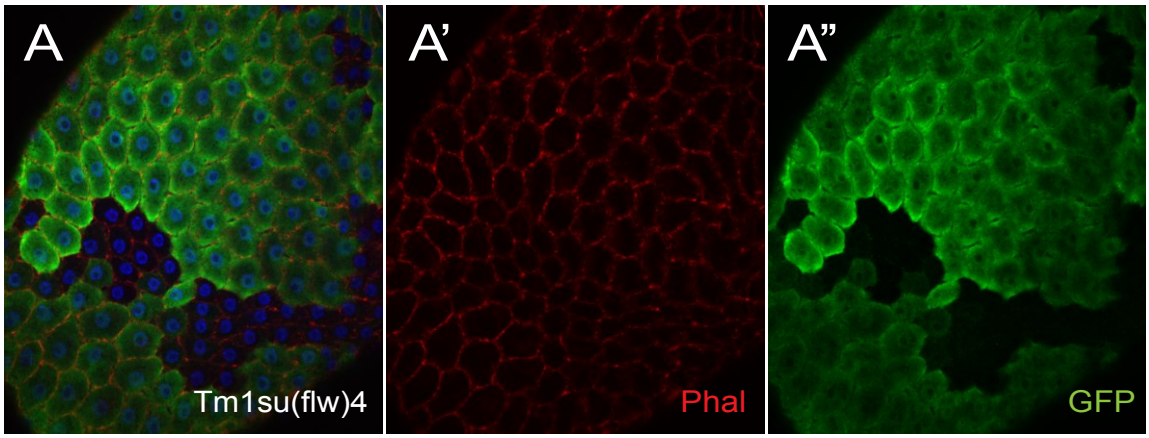
A
A'
A"
Tm1su(flw)4
Phal
GFP

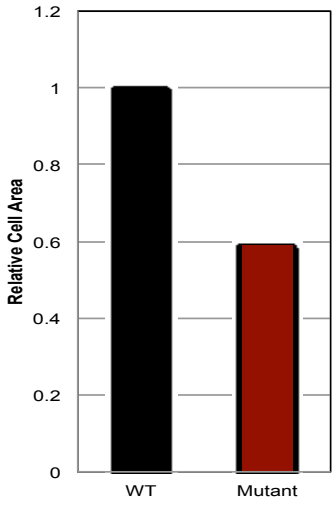
1.2
1
0.8
0.6
0.4
0.2
0
Relative Cell Area
WT
Mutant

Figure 20. Tm1 isoforms interact with each other to regulate their function and expression

(A) Overexpression of Tm1-A in subset of follicle cells (GFP positive cells) show slight increase in Tm1-I level. Since Tm1-I and Tm1-A antibodies do not cross react, this detection is due to more expression of Tm1-I caused by Tm1-A or more stabilized Tm1-I due to Tm1-A overexpression.

(B) Reduction or absence of Tm1-A by Tm1-A RNAi in RFP positive cells show reduction of Tm1-I (**B'**, GFP) compared to RFP negative wild type cells.

(C) Reduction or absence of Tm1-A in epithelial follicle cells excludes Tm1-L expression from the cell edge. $Tm1^{pz2299}$ homozygous mutant follicle cells are indicated by positive GFP. Tm1-L expression level in mutant cells is comparable to that of the wild type. While Tm1-L is expressed in the cell edge and in stress fibers of wild type follicle cells, Tm1-A reduced cells show loss of Tm1-L expression in the cell edge.

Scale bar, 10 μm

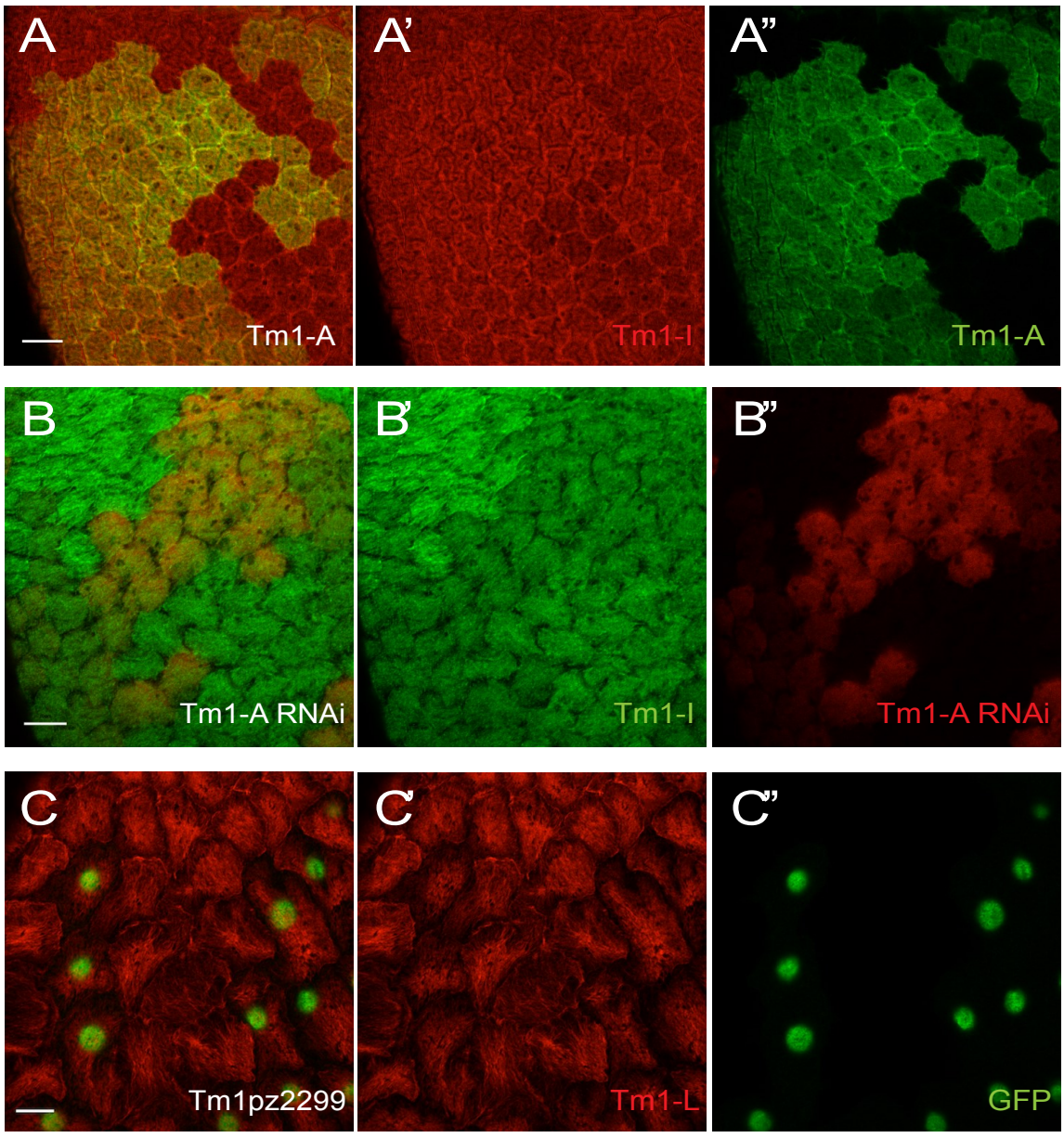
A
Tm1-A
A'
Tm1-I
A"
Tm1-A
B
Tm1-A RNAi
B'
Tm1-I
B"
Tm1-A RNAi
C
Tm1pz2299
C'
Tm1-L
C"
GFP

Chapter 3:
Tropomyosin interacts with Psidin to regulate actin dynamics

Introduction

Psidin, a conserved protein that regulates lamellipodia dynamics

Mutations in the gene *Psidin* (*Psid*) were discovered in our lab in a genetic screen of lethal mutations on chromosome 3R that cause border cell migration defects in mosaic clones (Kim et al., 2011). Psid is a 948 amino acid long protein, in which the only recognizable sequence motifs are a tetratricopeptide domain in the N-terminus and a partial coiled coil in the C-terminus. In cultured S2 cells, Psid overexpression enhanced lamellipodia dynamics, while knockdown of the protein reduced the dynamic activity. A similar phenotype was observed in MCF10A breast epithelial cells in a wound healing assay when the Psid human homolog C12orf30 was either knocked down or overexpressed.

Since Psid regulated actin dynamics, to gain further insight into its mechanism of action, we tested for genetic interaction of Psid with other actin regulatory proteins. Briefly, Psid was overexpressed in the border cells in the background of heterozygous for mutations in genes such as Rac, Cofilin, Slingshot, and Tropomyosin (Tm1). Among these genes, only mutations in Tm1 caused a border cell migration defect, with mutations in 27% to 50% of the stage 10 egg chambers. Genetic interactions have also been described between the yeast Psidin homolog called MDM20 and yeast Tropomyosin (Polevoda et al., 2003; Singer and Shaw, 2003).

Results

Tropomyosin and Psidin null border cells show rescue in border cell migration defect

Border cells mutant for *psid* showed approximately 80% migration defect. Tm1 mutant border cell analysis also showed 80% migration defect. Since Tm loss of function mutations enhanced the Psid overexpression phenotype in border cells, we tested whether Tm loss of function would suppress the Psid loss of function phenotype. Strikingly, when the level of both proteins was reduced simultaneously, the border cell migration defect was rescued (Figure 1). This result suggests that the two genes have antagonistic functions in regulating border cell migration.

The Psidin - actin interaction is disturbed in the presence of Tropomyosin

Since we observed a genetic interaction between Psid and Tm *in vivo*, we tested for their interaction using a biochemical assay. Using purified Psid and Tm-I proteins, we performed an actin co-sedimentation assay to see if the presence of either protein interfered with the other's binding to actin. First, we confirmed that both Tm-I and Psid bind to actin filaments in a F-actin pelleting assay. Second, we compared the level of Tm1-I in the actin pellet in the absence or presence of purified Psid. Interestingly, Tm1-I pelleted 3.5 fold less in the presence of Psid (Figure 2), showing that Psid interferes with Tm's binding to actin filaments.

Discussion

Drosophila border cell migration is a favorable, genetically tractable model system that allowed us to identify numerous genes and pathways that govern cell migration. Specifically, border cell specification, timing of their delamination, and their control of directionality have been identified (Pocha and Montell, 2014).

Cell migration has been highly investigated using cultured cells, and many actin-regulating factors that govern the actin dynamics in lamellipodia have been identified (Pollard and Borisy, 2003). However, it is not clear to what extent we can apply these finding *in vivo* because there are many more factors involved in a cellular environment. Fortunately, border cell migration, along with its developed live imaging technique, provides us with a wonderful *in vivo* system to study actin dynamics *in vivo*. Using this system, we have identified a conserved, but poorly characterized protein Psid. Psid binds to F-actin to regulate its dynamics *in vivo*. Altering its expression level affected protrusion dynamics in both border cells and S2 cells. In addition, the Psid human homolog was shown to have a similar phenotype in mammalian cells when the level was altered.

Our functional study of Psid showed that Psid and Tm1 have antagonistic functions in regulating the lamellipodia dynamics (Figure 3). Specifically, Psid and Tm1 showed genetic interactions when regulating actin dynamics during border cell migration. In a recent study, it was found that Psid is a regulator of *Drosophila* olfactory development (Stephan et al., 2012). When Psid was mutated, the growth cones of cultured primary neurons showed significantly smaller lamellipodia. Tm1 mutant neurons

alone did not have any detectable phenotype. However, the Psid mutant phenotype was suppressed by parallel reduction of Tm1, suggesting that Psid promotes actin dynamics by restraining Tm1 activity. These results suggest that Psid and Tm1 function antagonistically in various tissues in *Drosophila*. In addition, Psid has been shown to physically bind to the *Drosophila* catalytic subunit of N-acetyltransferase complex B (NatB;dNAA20). The complex is known to acetylate cytosolic proteins on their N terminus. Mutant *psid* that showed reduced binding to dNAA20 also showed reduced olfactory receptor neuron survival, implicating a dNAA20-dependent role of Psid during cellular functions. These studies suggest that Psid uses evolutionary conserved pathway to serve actin dynamics.

Which of the Tm1 isoforms is the Psid interacting with?

We observed that Tm1 and Psid show antagonistic functions during border cell migration by using available a Tm1 mutant line, $Tm1^{zcl0722}$. The mutant fly was made by random insertion of an artificial exon encoding GFP in the chromosome (FlyTrap). Because nothing was known about the mutant line, we did not know which Tm1 isoform was affected by the GFP insertion. However, recent generation of antibodies has allowed us to identify that $Tm1^{zcl0722}$ flies lacked isoforms Tm1-L and Tm1-A and almost no Tm1-I, making the line close to null. Preliminary data shows that border cells that are homozygous mutant for psid have slight elevation in Tm1-L level, but unchanged Tm1-A and Tm1-I levels. It would be interesting to test if any of the isoform specific mutations

or RNAi exhibits the same genetic interaction as $Tm1^{zcl0722}$, or if loss of all isoforms is necessary for the genetic effect.

Psid-Tm and other actin regulating proteins to regulate lamellipodial dynamics

A biochemical assay with Psid and Tm1 suggests a direct interaction in regulating actin filaments. However, as many *in vitro* studies suggest, there are many more proteins that possibly interact with tropomyosin, such as cofilin or the Arp2/3 complex (Blanchoin et al., 2001; Ono and Ono, 2002). Our analysis showed that a *psid* mutation and the *Drosophila* gene encoding cofilin, known as *twinstar*, interact genetically. However, Psid-cofilin interaction was not observed in the biochemical analysis, suggesting that the interaction is indirect. Perhaps Psid-mediated antagonism of Tm1 enhances cofilin's access to filaments and thus its activity. Psid-Tm1-cofilin interaction was also suggested by Stephan et al (Stephan et al., 2012). Taken together, these studies have enhanced our understanding of the complex regulation of actin dynamics *in vivo*.

Material and Methods

Drosophila Strains and Genetics

Mosaic clones were generated by crossing FRT82B, psid^{55D4} flies with hsp70-FLP; FRT82B, ubiGFP or hsp70-FLP; FRT82B, Arm-lacZ. Tm1^{zcl0722} or Tm1$^{su(flw)4}$ mutant mosaic clones were generated in the same way using FRT82B recombined mutant alleles. hsp70-FLP,tubGal4,UAS-GFP-nls; FRT82B, tubGal80 was used to positively mark the homozygous mutant border cells. To make the Psid and Tm1 double mutant line, FRT82B, Tm1^{zcl0722} was recombined with psid^{55D4} on the third chromosome. The flies were then crossed with hsp70-FLP; FRT82B, Arm-lacZ to make mosaic egg chambers. Heat shock at 37°C was performed for one hour, two times a day for three days; the ovaries were dissected 5 to 8 days after the heat shock.

Immunohistochemistry and Imaging

Ovaries were dissected in Schneider's medium (GIBCO) supplemented with 10% FBS (Sigma) and fixed for 15 minutes in 4% paraformaldehyde. After three, 15 minute washes with PBT (1x PBS, 0.1% Triton x-100) the egg chambers were blocked with PBT block (1x PBT, 5% goat serum) for 2 hours at room temperature or overnight at 4°C. B-gal antibody 1:2000, anti-Armadillo 1:50, anti-Tm1-L 1:5000, anti-Tm1-A, and anti-Tm1-I primary antibodies were incubated overnight. Fluor-conjugated goat anti-rabbit or anti-mouse IgG antibodies were used as the secondary antibodies (Molecular Probes).

Protein purification

To purify Psid, His-tagged Psid was expressed in S2 cells. 200ml culture containing 5 x 10^6 cell/ml was induced overnight with 1mM $CuSO_4$. Cells were harvested and washed with PBS followed by lysis in binding buffer (5mM imidazole, 20mM Tris-HCl (pH 8.0), 0.2% Triton-X 100, 150mM KCl, 5% Glycerol, 5mM 2-mercaptoethanol, 1:500 protease inhibitor cocktail (roche)) for 1hr at 4°C. The supernatant was allowed to flow through a His-bind column charged with Ni-NTA(Novagen), after which the protein was eluted with 200mM imidazole in binding buffer.

Full length Tm1-I was amplified using specific primers with Drosophila EST LD11194 as a template. The cloned product was inserted into pGEX vector and transformed into bacteria. Tm-I was induced using 0.8mM IPTG overnight at room temperature. Cells were harvested with GST-binding buffer (25mM Tris (pH7.5), 150mM KCl, 1mM EDTA, 1:500 protease inhibitor cocktail (roche)) and lysed by sonication. After centrifugation, the supernatant was allowed to flow through glutathione-agarose resin overnight at 4°C. Finally, the protein was eluted with 10mM glutathione in GST-binding buffer.

In vitro Actin co-sedimentation assay

Actin co-sedimentation assays were performed according to the manufacturer's protocol (Cytoskeleton). Briefly, 0.05 - 1µM Psid and 0.5µM Tm1 were incubated with 4µM F-actin for 1 hr in F buffer (5mM Tris-HCl pH 8.0, 0.2mM CaCl2, 50mM KCl, 2mM MgCl2, 1mM ATP). Beckman Airfuge (Beckman-Coulter) was used to centrifuge the

sample mixture at 150,000g for 1 hour. The supernatant and pellet were then separated for western blotting.

GST antibody 1:1000 (Cell signaling), Psid antibody 1:1000, and actin antibody 1:2000 (Sigma) were used to detect the proteins on Western blots.

References

Blanchoin, L., Pollard, T.D., and Hitchcock-DeGregori, S.E. (2001). Inhibition of the Arp2/3 complex-nucleated actin polymerization and branch formation by tropomyosin. Current biology : CB *11*, 1300-1304.

Kim, J.H., Cho, A., Yin, H., Schafer, D.A., Mouneimne, G., Simpson, K.J., Nguyen, K.V., Brugge, J.S., and Montell, D.J. (2011). Psidin, a conserved protein that regulates protrusion dynamics and cell migration. Genes & development *25*, 730-741.

Ono, S., and Ono, K. (2002). Tropomyosin inhibits ADF/cofilin-dependent actin filament dynamics. The Journal of cell biology *156*, 1065-1076.

Pocha, S.M., and Montell, D.J. (2014). Cellular and molecular mechanisms of single and collective cell migrations in Drosophila: themes and variations. Annual review of genetics *48*, 295-318.

Polevoda, B., Cardillo, T.S., Doyle, T.C., Bedi, G.S., and Sherman, F. (2003). Nat3p and Mdm20p are required for function of yeast NatB Nalpha-terminal acetyltransferase and of actin and tropomyosin. The Journal of biological chemistry *278*, 30686-30697.

Pollard, T.D., and Borisy, G.G. (2003). Cellular motility driven by assembly and disassembly of actin filaments. Cell *112*, 453-465.

Singer, J.M., and Shaw, J.M. (2003). Mdm20 protein functions with Nat3 protein to acetylate Tpm1 protein and regulate tropomyosin-actin interactions in budding yeast. Proceedings of the National Academy of Sciences of the United States of America *100*, 7644-7649.

Stephan, D., Sanchez-Soriano, N., Loschek, L.F., Gerhards, R., Gutmann, S., Storchova, Z., Prokop, A., and Kadow, I.C. (2012). Drosophila Psidin regulates olfactory neuron number and axon targeting through two distinct molecular mechanisms. The Journal of neuroscience : the official journal of the Society for Neuroscience *32*, 16080-16094.

Figure 1. Migration defect caused by Tm1 mutant border cells

(**A-C**) GFP positive cells are $Tm1^{su(flw)4}$ mutant border cells. (**D-F**) $Tm1^{zcl0722}$ is a GFP trap line that makes the mutant border cells marked with GFP. (**E**) Negative βGal shows the mutant border cells. (**G-I**) Psid-Tm double mutant border cell migration.

Yellow arrows point to border cells and white arrows point to centripetal cells indicating the egg chambers are at stage 10.

Scale bars, 50 μm

(**J**) Histogram of Tm1 mutant border cell migration defect and Psid-Tm1 rescue. Stage 10 egg chambers with no or incomplete border cell migration were counted. Red bar indicates no migration, yellow bar migrated less than 50%, blue bar migrated more than 50% but not complete, and green bar indicates complete migration. Similar migration defect was seen in Psid mutant border cells and in Tm1 mutant border cells (80%). However, border cells knocked down in both Psid and Tm1 showed slight rescue (60% complete migration).

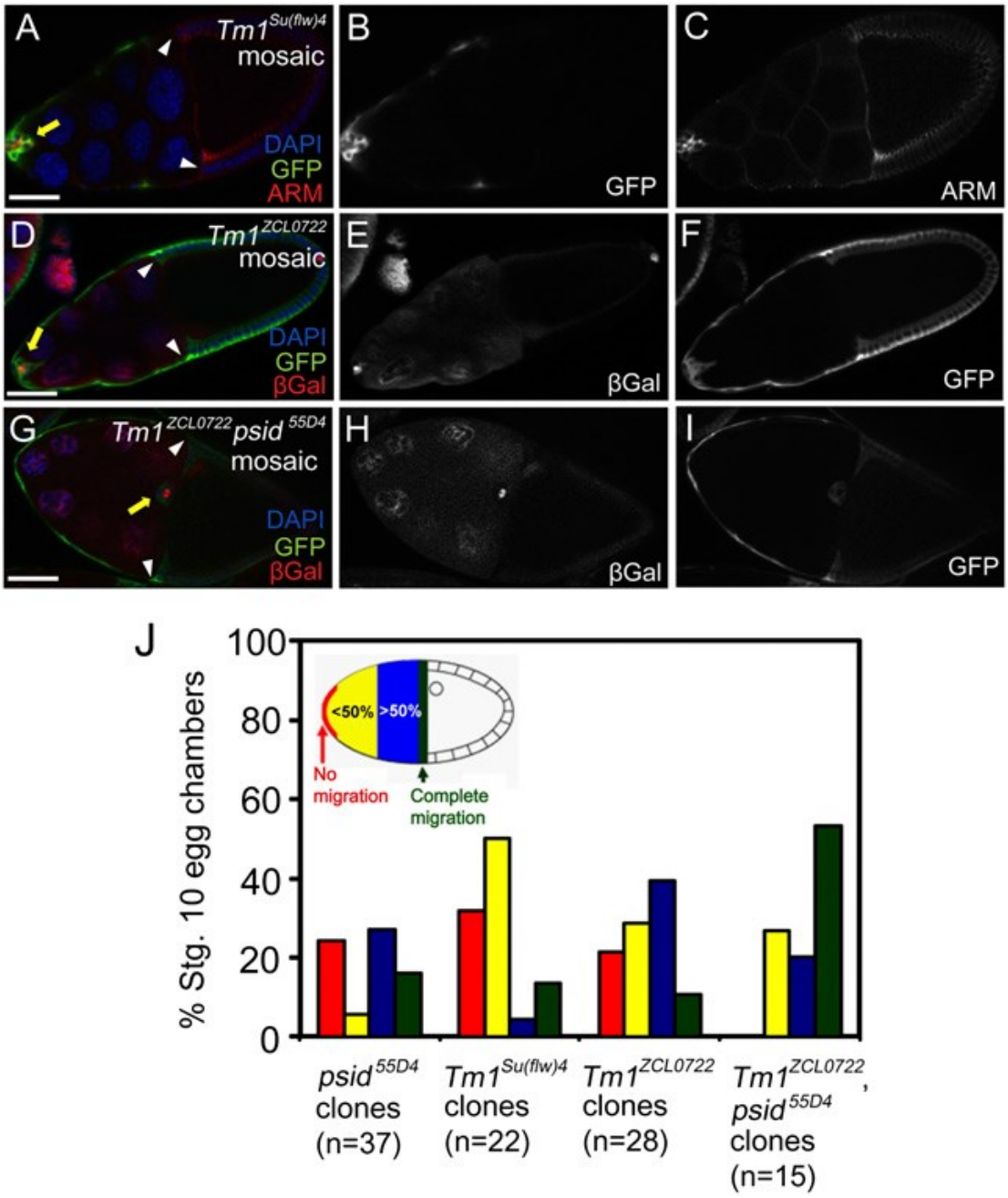
A
Tm1 Su(flw)4
mosaic
DAPI
GFP
ARM
B
GFP
C
ARM
D
Tm1 ZCL0722
mosaic
DAPI
GFP
βGal
E
βGal
F
GFP
G
Tm1 ZCL0722 psid 55D4
mosaic
DAPI
GFP
βGal
H
βGal
I
GFP
J
% Stg. 10 egg chambers
100
80
60
40
20
0
<50%
>50%
No migration
Complete migration
psid 55D4 clones (n=37)
Tm1 Su(flw)4 clones (n=22)
Tm1 ZCL0722 clones (n=28)
Tm1 ZCL0722 psid 55D4 clones (n=15)

Figure 2. Biochemical analysis of Psid and Tm1

(**A**) Purified GST-Tm-I binds to Actin filaments in an F-actin sedimentation assay.

(**B**) Purified Psid binds to actin filaments. The presence of Psid interferes with the binding of Tm-I to actin filaments. Each protein was visualized on Western blot using anti-actin, anti-GST and anti-Psid antibodies.

(**C**) Quantification of co-sedimentation assay. The representative is the average of four pelleting assay and error bars indicate the standard deviations.

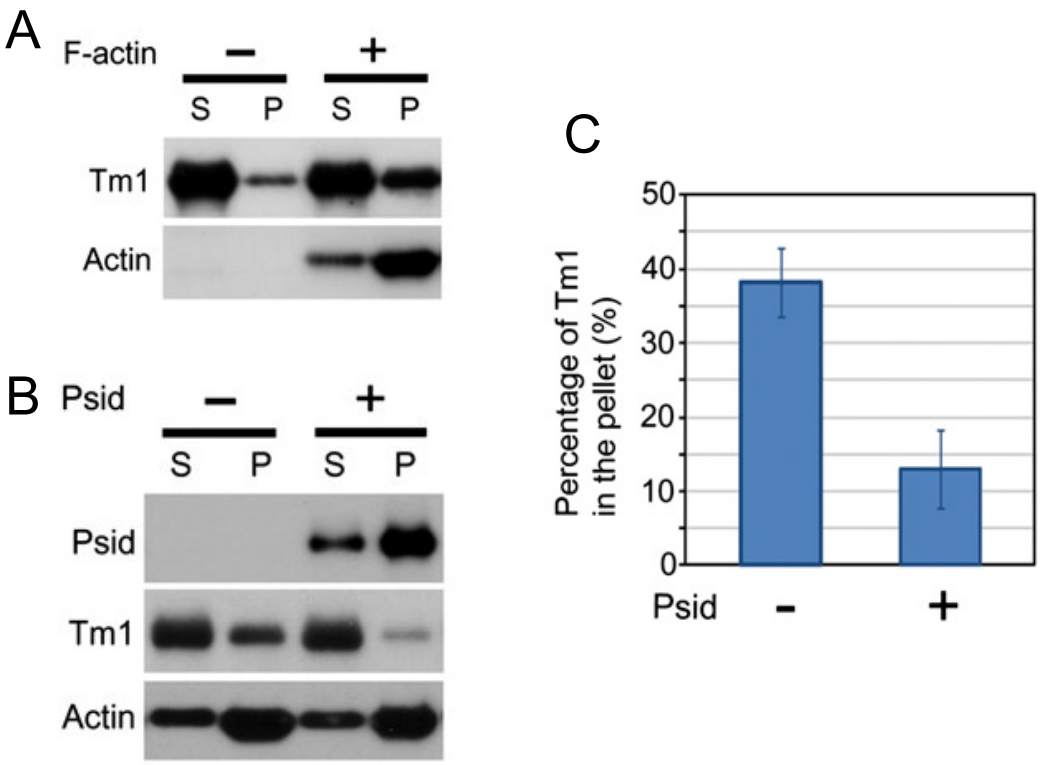
A
F-actin
–
+
S
P
S
P
Tm1
Actin
B
Psid
–
+
S
P
S
P
Psid
Tm1
Actin
C
Percentage of Tm1 in the pellet (%)
50
40
30
20
10
0
Psid
-
+

Figure 3. Schematic diagram of complementary distribution and antagonizing functions of Tm1 and Psid

Psid localizes to the lamellipodia (green) and binds to dynamic actin filaments (red) to promote assembly and disassembly. In the lamellipodia, presence of Psid inhibits binding of tropomyosin to the actin filaments, excluding its localization to the lamella area. Tropomyosin shows high concentration in the lamella where it binds to the actin filaments to stabilize them.

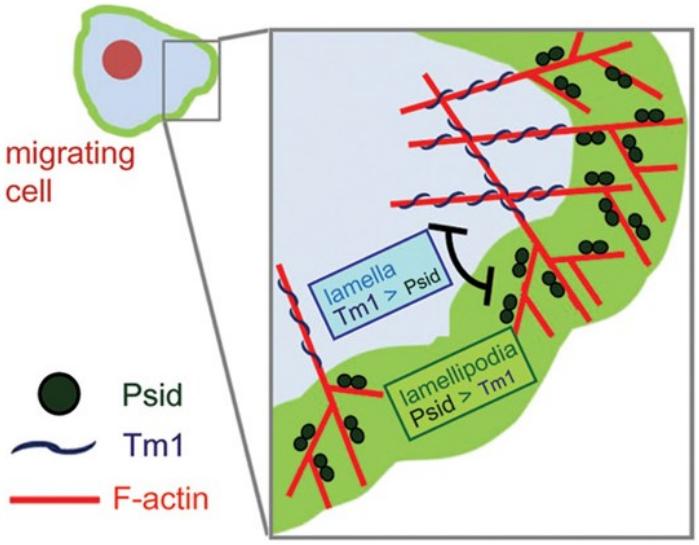

CURRICULUM VITAE

Aeri Cho
cho.aeri@gmail.com
650-243-1850

Education and Work Experience

Sep. 2008 - Present Ph.D. Candidate in the Department of Biological Chemistry
The Johns Hopkins University School of Medicine
Baltimore, Maryland
Advisor: Dr. Denise Montell.

Sep. 2006 – Jun. 2008 Research Technician
Dana Farber Cancer Institute
Boston, Massachusetts
Advisor: Dr. Shu-Ching Huang and Dr. Edward Benz

Sep. 2002 - May. 2006 B.A. Cum Laude in Biology
Amherst College
Amherst, Massachusetts

Honors and Awards

2006 Cum laude, Amherst College, Amherst, MA.

2013 Doreen J. Putrah Cancer Research Foundation Conference Fellowship

Publication

Byrne, R., Garnier, M., Han, K., Dowicki, M., Michael, N., Totty, N., ***Cho, A.***, Pettitt, T.R.,Wakelam, M.J.O., Larijani, B. and Poccia, D. "PLCg and Phosphoinositides are Highly Enriched in Membrane Vesicles Required for Nuclear Envelope Assembly." Cellular Signalling 19(5):913-22 (2007)

Zhou A, Ou AC, ***Cho A***, Benz EJ Jr, Huang SC "Novel splicing factor RBM25 modulates Bcl-x pre-mRNA 5' splice site selection." Mol Cell Biol 28(19):5924-36(2008)

Shu-Ching Huang, ***Aeri Cho***, Stephanie Norton, Eva S. Liu, Guang Yang, Anyu Zhou, Indira D. Munagala, Amittha Wickrema, Tang K. Tang, Edward J. Benz Jr. "Expression of

protein 4.1R: transcription and transcription coupled splicing regualation." Blood 114(19):4233-42(2009)

Kim JH, ***Cho A***, Yin H, Schafer DA, Mouneimne G, Simpson KJ, Nguyen KV, Brugge JS, Montell, DJ "Psidin, a conserved protein that regulates protrusion dynamics and cell migration." Genes Dev 25(7):730-41 (2011)

Manuscripts in preparation:

Aeri Cho, Tess Whitwam, Denise Montell. "Functional Analysis of Tropomyosin Isoforms *in vivo*".

Conference Presentation

Anyu Zhou, ***Aeri Cho***, Shu-Ching Huang, Edward J. Benz Jr. "A Novel Splicing Factor RBM25 in Erythroid Differentiation." ASH, Blood 110(11), 2007

SC Huang, ***A Cho***, SM Norton, ES Liu, EJ Benz Jr. " Alternative promoters govern protein 4.1R exon 2'/2 splicing decision" RNA, 2007

Aeri Cho and Denise Montell. "Functions of tropomyosin in vivo" The American Society of Cell Biology Annual Meeting, 2012

Aeri Cho and Denise Montell. "Functions of tropomyosin in vivo" Annual Drosophila Research Conference, 2014

Teaching experience

Fall 2005	Laboratory Teaching Assistant, Biology Department, Amherst College
Spring 2006	Teaching Assistant, Biology Department, Amherst College
Summer 2012	High School Intern Mentor, School of Medicine, Johns Hopkins University
Summer 2013 – Present	Undergraduate Research Assistant Mentor, MCDB. University of California, Santa Barbara

References

Denise Montell, Ph.D.
Professor, Department of Molecular, Cellular, and Developmental Biology
University of California, Santa Barbara
Bio II Rm 3127
Phone: (805) 893-3633
Email: denise.montell@lifesci.ucsb.edu

Doug Robinson, Ph.D.
Professor, Department of Cell Biology
Johns Hopkins University School of Medicine
725 North Wolfe St, Physiology 100
Baltimore, MD 21205
Phone: (410) 502-2850
Email: dnr@jhmi.edu

Shu-Ching Huang, Ph.D
Assistant Professor, Department of Medical Oncology
Harvard Medical School
450 Brookline Avenue,
Boston, MA 02215
Phone: (617) 632-6965
Email: shu-ching_huang@dfci.harvard.edu

Dominic Poccia, Ph.D.
Professor, Department of Biology
Amherst College
324 McGuire Life Sciences Building
Amherst, MA 01002
Phone: (413) 542-2198
Email: dlpoccia@amherst.edu